Nuclear factor I/B increases in prostate cancer to support androgen receptor activation

Jagpreet S. Nanda[1], Wisam N. Awadallah[1], Sarah E. Kohrt[2], Petra Popovics[1], Justin M. M. Cates[3], Janni Mirosevich[4], Peter E. Clark[5], Giovanna A. Giannico[3], and Magdalena M. Grabowska[1,2,6,7*]

[1] Department of Urology, Case Western Reserve University, Cleveland, OH

[2] Department of Pharmacology, Case Western Reserve University, Cleveland, OH

[3] Department of Pathology, Microbiology, and Immunology, Vanderbilt University Medical Center, Nashville, TN

[4] Department of Urology, Vanderbilt University Medical Center, Nashville, TN

[5] Department of Urology, Levine Cancer Center/Atrium Health, Charlotte, NC

[6] Department of Biochemistry, Case Western Reserve University, Cleveland, OH

[7] Case Comprehensive Cancer Center, Case Western Reserve University, Cleveland, OH

*Address correspondence to:

Magdalena M. Grabowska

2123 Adelbert Road

Wood Research Tower; RTG00

Cleveland, OH 44106

Phone: 216-368-5736

Email: mmg126@case.edu

Abstract:

Most prostate cancers express androgen receptor (AR), and our previous studies have focused on identifying transcription factors that interact with and modify AR function. We have shown that transcription factor nuclear factor I/B (NFIB) regulates androgen receptor (AR) activity and that its expression is decreased in the luminal cells of severe benign prostatic hyperplasia. To assess whether changes in NFIB expression are associated with prostate cancer progression, we immunostained a tissue microarray including normal, hyperplastic, prostatic intraepithelial neoplasia, primary prostatic adenocarcinoma, and castration-resistant prostate cancer tissue samples for NFIB, AR, and synaptophysin, a marker of neuroendocrine differentiation. We observed increased NFIB in the nucleus and cytoplasm of prostate cancer samples independent of Gleason score. We also observed strong NFIB staining in primary small cell prostate cancer. While increased NFIB nuclear and cytoplasmic staining were not predictive of biochemical recurrence, the ratio of cytoplasmic-to-nuclear NFIB staining was predictive of earlier biochemical recurrence once the analysis was adjusted for tumor margin status. We next assessed expression of NFIB in prostate cancer cell lines and detected several isoforms (62 kDa, 57 kDa, 49 kDa, and 39 kDa). Using nuclear and cytoplasmic fractionation, we observed NFIB predominantly in the nuclear fraction of prostate cancer cells with increased cytoplasmic expression seen in castration-resistant prostate cancer cell lines. Through transient transfection of AR and NFIB into the AR and NFIB low JEG-3 cells, followed by co-immunoprecipitation, we also observed a physical interaction between AR and NFIB. In order to understand the consequences of NFIB over-expression in prostate cancer, we generated vector or 3X-FLAG-NFIB-expressing androgen-dependent LNCaP and castration-resistant C4-2B cells (a LNCaP derivative cell line). While over-expression of NFIB did not increase AR expression, it did increase prostate specific antigen (PSA) production and PSA promoter activity. In summary, we have described the expression pattern of NFIB in prostate cancer and propose that one consequence of NFIB over-expression in AR-dependent prostate cancers is increased AR activity as measured by PSA induction.

51 **Introduction:**

52 Since most prostate cancers express androgen receptor (AR), even advanced prostate
53 cancer can be treated with androgen deprivation therapy[1]. Although these patients initially
54 respond to androgen deprivation therapy, disease progression typically occurs within 30 months
55 as these patients develop castration-resistant prostate cancer[2]. Castration-resistant prostate
56 cancer is treated with newer androgen deprivation therapies such as abiraterone acetate (a
57 steroidal CYP17A1 inhibitor[3]) and enzalutamide (a non-steroidal antiandrogen[4])[5,6]. However,
58 patients eventually progress on these second generation therapies as well and develop various
59 castration-resistant phenotypes.

60 Approximately 63% of castration-resistant prostate cancers maintain AR protein
61 expression[7]. In these tumors, AR signaling continues through multiple mechanisms including AR
62 over-expression, increased androgen production, and induction of constitutively active AR splice
63 variants (such as AR-V7)[8]. Prostate tumors can also escape androgen deprivation therapy by
64 bypassing AR signaling. One mechanism is neuroendocrine differentiation, whereby cells acquire
65 neuronal markers such synaptophysin and chromogranin A and sometimes lose AR expression
66 and activity. Focal neuroendocrine differentiation is observed in 85% of castration-resistant
67 prostate cancer patients[9] while 8-25%[7,10-12] of heavily treated prostate cancer patients, including
68 those treated with abiraterone or enzalutamide, will undergo neuroendocrine differentiation to
69 develop frank therapy induced neuroendocrine prostate cancer[11,13-19], which arises from the
70 transdifferentiation of the adenocarcinoma[10,15,18,20-23]. Foci of neuroendocrine differentiation and
71 therapy-induced neuroendocrine prostate cancers can be AR negative, have reduced AR activity,
72 and be less responsive to androgen deprivation therapy[11,24]. In mouse models, neuroendocrine
73 tumors can secrete neuronal factors, driving ligand-independent AR activation[25]. Another
74 mechanism of androgen-independence in castration-resistant prostate cancer cells is activation
75 of the fibroblast growth factor (FGF) pathway[7]. These “double negative” tumors lack both AR and

76 neuronal markers and represent 21% of enzalutamide and abiraterone resistant prostate
77 cancers[7].

78 Our previous studies have focused on identifying AR co-factors, based on the premise
79 that these co-factors might play critical roles in prostate cancer progression. Building on the
80 studies of Gao *et al*, which determined Forkhead box A1 (FOXA1) interacts with AR to drive
81 prostate-specific gene expression[26] and that Foxa1 is required for proper murine prostate gland
82 development[27] and maintenance[28], we identified NFI transcription factors (NFIA, B, C, X) as
83 FOXA1-interacting proteins that modulate AR-target gene expression[29]. Previous studies had
84 demonstrated a role for NFI family members in regulation of AR-responsive promoters[30,31], AR-
85 target gene expression in castration-resistant prostate cancer cells[32], and that NFI-consensus
86 sequences were associated with AR binding sites in prostate cancer cell lines and tissues[33]. Our
87 subsequent transient knockdown studies in androgen-dependent LNCaP cells demonstrated that
88 NFIB inhibits AR-target gene expression and that NFIB is frequently associated with AR binding
89 sites[34]. However, little was known about the expression pattern of NFIB in prostate cancer. We
90 therefore performed a tissue microarray study to define the expression of NFIB in prostate cancer
91 and determine whether its expression was associated with time to biochemical recurrence,
92 neuroendocrine differentiation, or castration-resistant disease.

93

94 **Methods:**

95 **Human prostate cancer samples**: Following Institutional Review Board (IRB) approval
96 (Vanderbilt: 140838; CRWU: 20180111), we analyzed a prostate cancer tissue microarray linked
97 with clinical data derived from the Urologic Outcomes Database at Vanderbilt University Medical
98 Center. This tissue microarray has been previously described[35]. Our cohort included samples
99 from 56 primary prostate cancer patients who had undergone radical prostatectomy and 8
100 castration-resistant prostate cancer patients who underwent tumor de-bulking procedures. The
101 tissue microarray included replicate 1 mm cores from prostatectomy specimens and included

102 normal prostatic tissue, benign prostatic hyperplasia (BPH), high-grade prostatic intraepithelial
103 neoplasia (HGPIN), and adenocarcinoma, Gleason patterns 3-5. The tissue microarray was
104 stained for NFIB (HPA003956, Sigma), AR (clone N-20, sc-816, Santa Cruz), synaptophysin
105 (Clone 2, BD Biosciences) as a marker of neuroendocrine differentiation, and hematoxylin and
106 eosin (H&E). Gleason score and immunohistochemistry staining was scored by a genitourinary
107 pathologist (GG). H&E stained array cores were scored as normal, BPH, HGPIN, or Gleason
108 pattern 3-5. Immunohistochemistry was scored by intensity (0 negative, 1 weak, 2 moderate, 3
109 strong) and distribution (0 negative, 1 <33%, 2 33-66%, and 3 >66%) in both nuclear and
110 cytoplasmic compartments of luminal cells (normal, BPH) or tumor cells (HGPIN, prostate cancer,
111 castration-resistant prostate cancer). A composite staining score was generated by summation of
112 intensity and distribution scores. For correlation analysis and staining by Gleason score, we
113 generated average values of duplicate cores. Unique cores and duplicate cores with differing
114 Gleason scores were treated as unique cores. We also generated average per patient scores,
115 averaging all cores to generate an average value for NFIB, AR, and synaptophysin across all
116 conditions. These patient scores were used to evaluate expression across disease states and
117 evaluate prostate cancer outcomes. Statistical analysis was performed using non-parametric
118 tests, detailed in the figure legends. Following IRB approval (Vanderbilt: 160346; CRWU:
119 20180111), we also analyzed 8 de-identified patient samples of primary small cell prostate cancer
120 obtained from O.U.R. Labs in 2005, with 1-3 needle biopsies available for analysis, as previously
121 described[36]. Images were acquired using an Olympus BX43 microscope and a SC50 5 mega
122 Pixel color camera and CellSens software. Immunohistochemistry images were white-balanced
123 using Adobe Photoshop by using a tissue-less point on the slide as the reference.
124
125 **Hematoxylin and Eosin staining:** Tissue microarray slides were soaked in xylenes (2 x 4
126 minutes), 100% ethanol (2 x 3 minutes), 95% ethanol (2 x 3 minutes), 70% ethanol (1 x 3 minutes),
127 and 50% ethanol (1 x 3 minutes). Slides were then washed in running tap water for 3 minutes and

128 dipped 10 times in de-ionized water. Slides were then placed in Harris hematoxylin (Richard Allan
129 Scientific) for 4 minutes, followed by 3 minutes in running tap water and 10 dips in de-ionized
130 water. Slides were then placed in Clarifier-2 (Richard Allan Scientific) for 45 seconds and rinsed
131 3 minutes in running tap water and 10 dips in de-ionized water. Rinsed slides were then placed
132 in Bluing Reagent (Richard Allan Scientific) for 30 seconds and again rinsed 3 minutes in running
133 tap water and 10 dips in de-ionized water. Slides were then placed in eosin-phloxine working
134 solution (780ml 95% ethanol, 40ml 1% eosin Y in distilled water, 10ml 1% phloxine B in distilled
135 water, and 4ml glacial acetic acid) for 2 minutes, and washed through 5 100% ethanol baths, 10
136 dips each before finally being dehydrated in xylenes (3 x 4 minutes). Slides were cover-slipped
137 with Cytoseal 60.
138
139 **Immunohistochemistry:** All slides and antibody stains were processed the same day, with
140 developing times set by positive controls. Tissue microarray slides were soaked in xylenes (2 x 5
141 minutes), 100% ethanol (2 x 2 minutes), 95% ethanol (2 x 2 minutes), 70% ethanol (1 x 2 minutes),
142 50% ethanol (1 x 2 minutes). Slides were then washed in running tap water for 3 minutes and
143 placed in a container with citric acid-based antigen unmasking solution (H-3300, Vector). Slides
144 were then placed in a pressure cooker and cooked on high pressure for 25 minutes. Following
145 pressure release, slides were allowed to cool for 25 minutes prior to subsequent steps. Slides
146 were washed in 1 X PBS (3 x 10 minutes). Endogenous peroxidase activity was blocked with a
147 20-minute incubation of slides in peroxidase blocking solution (2.5ml of 30% hydrogen peroxide
148 into 250ml methanol). Slides were again washed in 1X PBS (3 x 10 minutes). The tissue
149 microarray was outlined with a PAP pen, and blocking solution (50µl of horse serum in 3 ml PBS)
150 was added to slides for 30-minutes at room temperature. Blocking solution was removed and
151 primary antibodies (1:1000) were added to each slide and incubated at 4°C overnight. In the
152 morning, slides were washed in 1X PBS (3 x 10 minutes) before secondary antibody (1: 200,
153 Vector) was added for an hour at room temperature. While slides were washed in 1X PBS (3 x 10

154 minutes), A and B components (2 drops A, 2 drops B into 5 ml PBS, VECTASTAIN Elite ABC
155 HRP Kit) were combined to incubate for 30 minutes. AB solution was then added to slides and
156 incubated at room temperature for 60 minutes, followed by washes in 1 X PBS (3 x 10 minutes).
157 Slides were then developed with Liquid DAB+ Substrate Chromogen System (1 drop DAB+ per
158 ml of buffer, DAKO), quenched with water and counterstained as follows. Positive controls
159 (prostate for AR, NFIB, brain for synaptophysin) were used to set the exposure time, and all slides
160 in an antibody series were incubated for the same amount of time in DAB. Slides were washed
161 for 5 minutes in running tap water and then were placed in Harris hematoxylin (Richard Allan
162 Scientific) for 30 seconds, followed by 1 minute in running tap water and 10 dips in de-ionized
163 water. Slides were then dipped in Clarifier-2 for 3 times and rinsed 1 minute in running tap water
164 and 10 dips in de-ionized water. Rinsed slides were then placed in Bluing Reagent (Richard Allan
165 Scientific) for 10 dips and again rinsed 1 minute in running tap water and 10 dips in de-ionized
166 water. Slides were then dipped 10 times in 70% ethanol and dehydrated through 5 100% ethanol
167 baths, 10 dips each before finally being dehydrated in xylenes (3 x 4 minutes). Slides were cover-
168 slipped with Cytoseal 60.
169
170 **Cell lines:** LNCaP (clone FGC, CRL-2876), JEG-3 (HTB-36), 22RV1 (CRL-2505), PC-3 (CRL-
171 1435), and DU145 (HTB-81) cells were purchased from American Type Culture Collection
172 (ATCC). C4-2B[37] cells were provided by Drs. Ruoxiang Wu and Leland Chung (Cedars-Sinai).
173 LNCaP, C4-2B, and 22RV1 were cultured in 10% premium fetal bovine serum (FBS, Atlanta
174 Biologicals S11150) in RPMI 1640 + L-glutamine (Gibco). JEG-3 and DU145 cells were cultured
175 in 10% FBS in MEM + Earle's salts and L-Glutamine (Gibco). PC-3 cells were cultured in 10%
176 FBS in F-12K Kaighn's modification + L-Glutamine (Gibco). BHPrS-1, , NHPrE-1, and BHPrE-1
177 cells were provided by Dr. Simon Hayward (NorthShore Research Institute)[38,39]. BHPrS-1 cells
178 were maintained in RPMI supplemented with 5% FBS and NHPrE-1 and BHPrE-1 cells in
179 F12/DMEM 1:1 medium containing 5% FBS, 1% Insulin-Transferrin-Selenium supplement, 10

180 ng/ml epidermal growth factor, 0.4% bovine pituitary extract and 1% antibiotic-antimycotic mix (all
181 from Gibco). 3D cultures of NHPrE-1 and BHPrE-1 cells were established in 8-well chamber slides
182 by plating 2,000 cells/well in medium containing 2% (vol/vol) Matrigel on top of an undiluted layer
183 of Matrigel. These cultures were grown for 9 days and cells were released from Matrigel using
184 Corning Cell Recovery Solution to prepare cell lysates for western blot analysis.
185
186 **Plasmids:** pCMV6-Entry (vector) and pCMV6-NFIB-myc-DDK (RC231240) were purchased from
187 Origene. The AR construct, p5HbHAR-A, used to generate AR-V7 and AR-V9[40], was provided by
188 Dr. Scott Dehm (University of Minnesota). The PSA-EP-luciferase[26] construct was provided by
189 Dr. Robert Matusik (Vanderbilt University Medical Center) and the SV40-renilla construct was
190 purchased from Promega (pRL-SV40, E2231).
191
192 **Western blotting:** Proteins from cell lines were lysed in ice-cold RIPA buffer (120 mM NaCl, 50
193 mM Tris (pH 8.0), 0.5% NP-40 and 1 mM EGTA) containing 1 mM phenylmethylsulphonyl fluoride,
194 1 mM sodium orthovanadate, 0.1 μM aprotinin and 10 μM leupeptin and kept on ice for one hour.
195 Supernatants were collected by centrifugation at 13,750 rpm for 20 min at 4°C. Protein
196 concentration was quantified and equal amounts of protein were added to 2X SDS loading buffer
197 with 5% beta-mercaptoethanol. Nuclear and cytoplasmic extracts of LNCaP, C4-2B, 22RV1,
198 JEG-3, DU-145 and PC3 cells were prepared using NE-PER Nuclear and extraction reagents
199 (Thermoscientific, 78833). Equal amounts of cytoplasmic and nuclear protein extracts were
200 resolved on NuPAGE 4-12% Bis-Tris Gels and transferred to nitrocellulose membranes.
201 Membranes were blocked in 5% skimmed milk in TBS/0.1% Tween-20 (TBST) for 1 hour at room
202 temperature followed by incubation overnight at 4°C with indicated antibodies NFIB (HPA003956,
203 rabbit antibody, 1:1000 dilution, Sigma); AR (ab74272, rabbit antibody, 1:1000 dilution, Abcam);
204 lamin B1 (ab133741, rabbit antibody, 1:2000, Abcam); GAPDH (AM4300, mouse antibody,
205 1:5000, Invitrogen) and α-tubulin (ab7291, mouse antibody, 1:5000, Abcam). GAPDH was used

206 as cytoplasmic loading control whereas lamin B1 was nuclear loading control. Following
207 secondary antibody incubation, proteins of interest were visualized using ECL detection reagent
208 (GE Healthcare, RPN3243). Images were acquired using a Bio-Rad Chemi Doc. Molecular
209 weights were calculated using Bio-Rad Image Lab. Average molecular weights of NFIB were
210 determine from three independent experiments.
211
212 **Transient transfections:** 400,000 (JEG-3, LNCaP, 22RV1) or 300,000 (C4-2B) cells were plated
213 in 6-well plates. After overnight recovery, cells were transiently transfected with Silencer Select
214 Pre-Designed siRNAs either as negative control (non-targeting, Silencer Select Negative Control
215 No. 1 and 2 siRNA) or NFIB-targeting siRNA constructs (Thermofisher, s9494, s9496) using 30
216 pmol of siRNA in 9 µl of Lipofectamine RNAi Max. Cells were transfected for 72 hours, collected,
217 and analyzed by Western blotting as above.
218
219 **Co-immunoprecipitation:** $2.5 \cdot 10^6$ JEG-3 cells were seeded per plate in 10 cm dishes. After 10
220 hours, cells were transfected with 10 µg of empty, NFIB (variant 2), full length AR plasmid alone,
221 or in combination using polyethylenimine (PEI) (Polysciences, Warrington, PA, USA) at a ratio of
222 3:1. Cells were washed with 1X PBS 48 hours after transfection and dislodged with a cell scraper.
223 Cells were lysed in 500 µL of ice-cold RIPA buffer (120 mM NaCl, 50 mM Tris [pH 8.0], 0.5%
224 NP-40 and 1 mM EGTA) containing 1 mM phenylmethylsulphonyl fluoride, 1 mM sodium
225 orthovanadate, 0.1 µM aprotinin and 10 µM leupeptin and kept at 4°C on a rotospin for 1 hr.
226 Supernatants were collected by centrifugation at 13,750 rpm for 20 min at 4°C. 80 µL of lysate
227 was kept aside for protein quantification and analysis of input samples. The remainder of the
228 lysate was used for preclearing by incubating them with 30 µL of equilibrated Pure Proteome TM
229 Protein A Magnetic beads (LSKMAGA10) for 1 hour on ice. Then 4 µL of NFIB antibody from
230 Sigma (HPA003956) was added per precleared sample for immunoprecipitation and kept on
231 rotospin overnight at 4°C. The next day, 50 µL of equilibrated Protein A Magnetic beads were

232 added to each sample and incubated for 6 hours before washing three times with RIPA buffer.
233 Proteins were eluted with 60 µL of 2X SDS PAGE loading buffer with 5% beta-mercaptoethanol.
234 Input and bead samples were heated at 70°C for 13 min and analyzed by SDS PAGE and
235 immunoblotting.
236
237 **Stable Expression of 3X-FLAG NFIB in LNCaP and C4-2B cells:** N-terminally 3X Flag tagged
238 human NFIB (variant 2, NM_001190738.1) was PCR amplified from GFP-NFIB plasmid (Origene,
239 RG231240) and cloned into BamH1 and Sal1 sites of pBABE-puro, a retroviral vector (gift from
240 Hartmut Land, Jay Morgenstern, and Bob Weinberg [Addgene plasmid # 1764;
241 http://n2t.net/addgene:1764; RRID:Addgene_1764][41]. Clones were verified by sequencing before
242 use. Stable LNCaP and C42B cells lines were generated by stable expression of pBABE (vector)
243 or 3X-Flag NFIB by retroviral infection. Briefly, $2 \cdot 10^6$ GP2-293 cells were seeded per dish in 10
244 cm dishes containing DMEM and 10% FBS for 18-20 hours. Cells were then transfected with 12
245 µg of pBABE-puro or pBABE-puro Flag NFIB and pCMV-VSV-G plasmids at a ratio of 3:1 using
246 polyethylenimine (PEI) (Polysciences, Warrington, PA, USA). pCMV-VSV-G was a gift from Bob
247 Weinberg (Addgene plasmid # 8454; http://n2t.net/addgene:8454 ; RRID:Addgene_8454)[42].
248 Virus-enriched medium was collected 48 and 96 hours after transfection and centrifuged at 800 x
249 g for 10 min and used to infect LNCaP or C4-2B cells in 60-mm dishes with 0.5 mL of RPMI1640
250 medium containing 10% FBS. Two rounds of retrovirus infections were performed on 2 sequential
251 days in presence of 4.0 µg/mL of hexadimethrine bromide (Sigma). Cells were re-plated into 10
252 cm dishes 48 hours after the second infection and allowed to grow in presence of puromycin
253 containing RPMI 1640 with 10% FBS for 4 days before they were used for further experiments. 2
254 µg/mL and 4 µg/mL of puromycin was used to select stable LNCaP and C4-2B cells. Whole cell
255 extracts from stable cells were checked for 3X-FLAG NFIB expression by western blotting using
256 FLAG M2 antibody (F1804, mouse antibody, 1:3000, Sigma).
257

258 **Cytokine array:** LNCaP and C4-2B vector and NFIB over-expressing cell lines were grown in
259 complete media. Cells were collected, lysed, and whole cell extracts were prepared as above.
260 Whole cell extracts were then applied to the Proteome Profiler Human XL Cytokine Array Kit per
261 manufacturer's instructions (R&D Systems). The Proteome Profiler Human XL Cytokine Array
262 includes 105 cytokines blotted in duplicate. Images were acquired as above, with each cell line
263 (vector and NFIB) imaged at the same time. Dotblot analysis was performed using ImageJ[43-45].
264 First, the background was subtracted (rolling ball radius of 25 pixels) and the imaged inverted. A
265 circle was drawn around the positive control and integrated density was measured of each visible
266 dot plus two negative control areas. The difference between the integrated density of each dot
267 and the negative control was considered the true integrated density. For analysis by cell line, we
268 adjusted for membrane variability by generating a ratio of vector-to-NFIB positive controls. We
269 multiplied all NFIB values by this number to generate an adjusted integrated density comparable
270 between the cell lines. For analysis between cell lines, we divided each integrated density value
271 by the average positive control value for each cell line. This generated a percentage of the positive
272 control signal, and allowed us to compare the amount of cytokine between all four cell lines.
273 Graphs include an average of the two adjacent dots and are provided to aid with data
274 interpretation. No statistical analysis was performed.
275
276 **Luciferase reporter assays:** LNCaP and C4-2B vector and NFIB overexpressing cells were
277 plated 150,000 or 70,000 cells per well of a 24-well plate, respectively. Cells were transfected
278 with prostate-specific enhancer-promoter construct (PSA-EP)-luciferase[26] and SV40-renilla
279 constructs (transfection control) in Lipofectamine 2000 for 24 hours. Cells were then collected,
280 lysed, and luciferase and renilla expression was quantified using the Dual-Reporter assay system
281 (Promega) using a SpectraMax ID3 plate reader with a dual injection system. Luciferase data was
282 then normalized to renilla and then vector cells.
283

284 **Statistical analysis:** Statistical analysis was performed using SPSS 24 (IBM) or GraphPad Prism
285 and utilized non-parametric tests, with P values smaller than 0.05 considered significant. Dot plots
286 are overlaid with mean with standard deviation.
287
288 **Results:**
289 Our previous study of a small cohort of patients demonstrated that NFIB was frequently
290 lost in the luminal cells of patients with severe benign prostatic hyperplasia[34]. To determine
291 whether this was also true in prostate cancer patients, we stained a tissue microarray and several
292 core biopsies with an antibody against NFIB (Figure 1, Supplemental Figure 1A, B), which we had
293 previously validated in *Nfib* knockout mouse tissues[34]. In order to determine whether changes in
294 NFIB expression were associated with changes in AR or acquisition of neuroendocrine features,
295 we also stained the tissue microarray for synaptophysin. Staining was then scored by a board-
296 certified genitourinary pathologist (GG).
297 Using an average patient score, we compared the expression of NFIB, AR, and
298 synaptophysin in normal prostate and prostate cancer (Figure 2 A-C). NFIB was over-expressed
299 in the nucleus ($P = 0.0259$) and cytoplasm ($P < 0.0001$) of cancer tissues versus patient matched
300 normal prostate tissues. While AR was not over-expressed in the nucleus, cytoplasmic AR was
301 increased in prostate cancer tissues versus normal prostate ($P < 0.0001$). Synaptophysin staining
302 was limited to the cytoplasm and cell membrane, and also increased in prostate cancer tissues
303 ($P < 0.0001$).
304 To evaluate whether NFIB, AR, and synaptophysin expression corresponded with
305 Gleason grade, we generated average scores per each unique core. There was no statistically
306 significant difference between Gleason grade 3 versus 4 or Gleason grade 3 versus 5 for AR,
307 NFIB, or synaptophysin (Figure 2 D-F). Using these values, we also correlated the expression of
308 nuclear and cytoplasmic NFIB with AR and synaptophysin. In primary prostate cancer samples,
309 nuclear and cytoplasmic NFIB levels were positively correlated (Spearman rho = 0.305, P =

310 0.001), suggesting that NFIB expression increases in both compartments and that increasing
311 cytoplasmic expression is not due to a shift in cytolocalization (Supplemental Figure 2A). Nuclear
312 NFIB was also positively correlated with nuclear AR (Spearman rho = 0.419, P < 0.0001).
313 Cytoplasmic NFIB was positively correlated with nuclear AR (Spearman rho = 0.248, P = 0.006),
314 cytoplasmic AR (Spearman rho = 0.447, P < 0.0001), and synaptophysin (Spearman rho = 0.464,
315 P < 0.0001). The positive correlation of cytoplasmic NFIB with synaptophysin remained intact
316 whether we examined all prostate cancer tissues (primary and castration-resistant) or castration-
317 resistant only (Supplemental Figure 2B, C).

318 We also examined whether NFIB expression correlated with biochemical recurrence in 51
319 primary prostate cancer patients for who we had biochemical recurrence data. For these patients,
320 we again used the average NFIB nuclear and cytoplasmic score (Figure 3A). Nuclear and
321 cytoplasmic NFIB staining did not correlate with biochemical recurrence (Figure 3B, C). However,
322 when we examined a ratio of cytoplasmic and nuclear NFIB, we found a high ratio of cytoplasmic-
323 to-nuclear NFIB predicted earlier biochemical recurrence (P = 0.058; hazard ratio 2.864; 95% CI
324 0.966 – 8.491; Figure 3D, E), an effect that achieved statistical significance when surgical
325 resection margin status was accounted for in the Cox regression model (P = 0.004; hazard ratio
326 8.930; 95% CI 1.989 – 40.086; Figure 3F). There was no difference in cytoplasmic-to-nuclear
327 NFIB by Gleason grade or tumor stage (Supplemental Figure 3A)

328 To more fully explore NFIB expression in the normal and diseased prostate, we compared
329 NFIB average patient scores in unmatched patient samples, using unpaired analysis (Figure 4A,
330 Supplemental Figure 3 B-D). Consistent with our previous report, NFIB was lost in the nucleus of
331 hyperplastic areas[34], with low levels of cytoplasmic NFIB observed (Supplemental Figure 3A).
332 While there was no statistically significant difference between nuclear NFIB staining in primary
333 prostate cancer versus normal tissue or castration-resistant prostate cancer, cytoplasmic NFIB
334 was again increased in primary prostate cancer versus normal prostate tissue (P < 0.0001) but
335 not castration-resistant samples. While nuclear AR expression was unchanged, cytoplasmic AR

336 was decreased in normal prostate samples (P = 0.0002) and increased in castration-resistant
337 samples (P = 0.0038), versus primary prostate cancer (Figure 4B). Synaptophysin expression
338 was also significantly lower in normal prostate tissue versus prostate cancer (P = 0.007), but there
339 was no significant difference between primary prostate cancer and castration-resistant (Figure
340 4C).

341 Because only one of our castration-resistant prostate cancer cases satisfied our criteria
342 for neuroendocrine features (loss of AR, strong synaptophysin staining), we also analyzed a
343 limited number (n=8) of primary small cell prostate cancer core biopsies. Of these, 7 (88%)
344 showed strong nuclear NFIB staining (Supplemental Figure 1B). Small cell prostate cancer cells
345 have limited cytoplasm, so NFIB expression was not scored.

346 In order to evaluate whether established prostate cancer cell lines recapitulate the nuclear
347 and cytoplasmic expression of NFIB, we performed nuclear and cytoplasmic protein isolation from
348 prostate cancer cell lines. We examined androgen-dependent (LNCaP), castration-resistant (C4-
349 2B, 22RV1), and AR-independent (DU-145, PC3) prostate cancer cells. As a control, we used
350 JEG-3 cells which express limited NFIB based on previous reports and gene expression
351 analysis[29,46]. NFIB isoforms were found in all cell lines (Figure 5A), including benign stromal and
352 epithelial cells (Supplemental Figure 4A). NFIB exists as four isoforms in most prostate cancer
353 cell lines, at 62 kDa, 57 kDa, 49 kDa, and 39 kDa (Supplemental Figure 4B).

354 In order to verify which of these bands are true NFIB bands, we performed transient
355 transfections and over-expression studies. First, we transiently transfected PC-3 cells with NFIB
356 over-expression or NFIB-knockdown constructs and compared which bands were impacted
357 (Supplemental Figure 4C). In PC-3 cells, transient NFIB over-expression gave rise to a 53kDa
358 band. Importantly, all other putative NFIB isoforms increased as well (62 kDa, 57 kDa, 49 kDa
359 and 39 kDa), suggesting that NFIB auto-regulates its own expression. Transient transfection of
360 an NFIB-targeting siRNA also decreased expression of the 62kDa, 57 kDa, and 49 kDa bands,
361 suggesting that these bands do indeed represent NFIB. We also expanded this analysis to JEG-3,

362 LNCaP, C4-2B, and 22RV1 cells. In the LNCaP and C4-2B cells, transient knockdown abrogated
363 expression of both the 57 kDa and 49 kDa bands (Supplemental Figure 4D). Neither of these
364 were expressed in JEG-3 cells. In 22RV1 cells, NFIB knockdown also decreased expression of
365 the 62 kDa band, which was not impacted in JEG-3, LNCaP, or C4-2B cells. However, as this
366 band increased in response to NFIB over-expression and decreased in both 22RV1 and PC-3
367 cells in response to transient knockdown, we consider it an NFIB isoform. Finally, although the
368 39 kDa band was not decreased in response to transient knockdown in the prostate cancer cells,
369 its expression was limited in JEG-3 cells, and its expression increased in the NFIB-overexpressing
370 cell lines.

371 Because cytoplasmic NFIB expression in prostate cancer patient tissues was higher in
372 castration-resistant samples, we compared NFIB localization in LNCaP, C4-2B, and 22RV1 cells
373 (Figure 5B). In LNCaP cells, which are androgen-dependent, NFIB is largely in the nucleus, but
374 as cells progress to castration resistance in C4-2B cells, NFIB expression increases in both the
375 nuclear and cytoplasmic fractions. These levels are even more pronounced in the unrelated
376 castration-resistant prostate cancer cell line, 22RV1. Similarly, cytoplasmic AR expression
377 increased in both castration-resistant prostate cancer tissue and cell lines.

378 Since AR and NFIB are frequently co-occupying the same cellular compartment, AR and
379 NFIB co-occupy the same genomic regions in a prostate cancer cell line, and our previous studies
380 determined NFIB regulates AR-target gene expression[29,34], we evaluated whether NFIB and AR
381 can interact directly by transfecting NFIB and AR into JEG-3 cells, which express low levels of
382 NFIB. Indeed, in transient transfection co-immunoprecipitation experiments, NFIB and AR co-
383 immunopurify (Figure 5C).

384 To start elucidating the roles of NFIB in primary and castration-resistant prostate cancer,
385 we turned to well-defined *in vitro* models. We focused on two related cell lines: LNCaP cells are
386 androgen-dependent, while their bone-homing metastatic derivative C4-2B cells are castration-
387 resistant. We generated pBABE (vector) or 3X-FLAG-NFIB over-expressing LNCaP and C4-2B

388 cells (Figure 5D). Cell lines were positive for the Flag-tagged NFIB (53 kDa) and also showed
389 increased endogenous NFIB expression (53 kDa, 49 kDa, 39 kDa). This observation was
390 consistent with our previous experiments, where transient over-expression of NFIB induced
391 increased expression of multiple NFIB isoforms in PC-3 cells (Supplemental Figure 3C).
392 Importantly, only one band was detected by the Flag antibody, indicating NFIB is not degraded,
393 but rather exists as a series of isoforms. We did not observe any changes in AR protein expression
394 in these cells (Figure 5D).

395 To examine some of the downstream targets of NFIB over-expression, we compared
396 cytokine expression using proteome profiling. The arrays included 102 cytokines and secreted
397 proteins, including prostate specific antigen (PSA) and IL-6, which has been implicated in
398 neuroendocrine differentiation[47-50]. In LNCaP cells, NFIB over-expression dramatically induced
399 PSA, along with DPPIV, GDF-15, and IGFBP-2; angiogenin, EGF, cystatin C, resistin,
400 pentraxin-3, and CD71 were also induced, but to a smaller extent (Figure 6A, B). In C4-2B cells,
401 over-expression of NFIB induced small changes in angiogenin and EGF. Importantly, over-
402 expression of NFIB in LNCaP cells resulted in expression of PSA, GDF-15, and IGFBP-2
403 comparable to their castration-resistant derivative (Figure 6C).

404 To confirm that PSA expression is indeed regulated by NFIB, we performed reporter
405 assays in our two cell lines using a prostate specific antigen enhancer and promoter (PSA-EP[26])
406 element linked to luciferase. In both LNCaP and C4-2B cells, over-expression of NFIB resulted in
407 increased PSA-EP reporter activity (Figure 6D, E), increasing AR activity by 1.2 fold and 1.4 fold
408 versus parental cell lines respectively ($P < 0.01$).

409

410 **Discussion:**

411 The goal of our study was to define the expression of NFIB in prostate cancer with respect
412 to AR and synaptophysin and to begin to unravel the relationship between NFIB and prostate
413 cancer progression. We analyzed a tissue microarray composed of cores including normal, BPH,

414 prostate cancer, and castration-resistant prostate cancer tissues samples. On a matched per-
415 patient basis, NFIB is over-expressed in both the nuclear and cytoplasmic compartments in
416 primary prostate cancer versus normal prostate tissue. Importantly, increasing nuclear NFIB
417 expression corresponds with increasing cytoplasmic expression, suggesting that NFIB continues
418 to occupy the nucleus in prostate cancer. Indeed, there is no statistically significant difference
419 between primary and castration-resistant prostate cancer in terms of nuclear or cytoplasmic NFIB
420 expression.

421 There also was not a significant difference between NFIB expression in either
422 compartment when compared by Gleason pattern, enabling us to evaluate the utility of NFIB as
423 predictor of biochemical recurrence, independent of Gleason grade. While nuclear NFIB or
424 cytoplasmic NFIB expression alone could not predict biochemical recurrence, a higher ratio of
425 cytoplasmic-to-nuclear NFIB predicted earlier time to biochemical recurrence when we accounted
426 for surgical margin status in the Cox regression analysis. This observation is exciting, but a
427 limitation to our analysis is the sample size as well as the challenge of generating both a
428 cytoplasmic and nuclear score for each patient. While these limitations limit the utility of NFIB as
429 biomarker of biochemical recurrence, these observations do suggest NFIB plays an interesting in
430 prostate cancer biology.

431 Consistent with our human tissue data, NFIB is expressed in the nuclear and cytoplasmic
432 fractions of prostate cancer cells. As in castration-resistant prostate cancer, castration-resistant
433 prostate cancer cell lines have increased levels of NFIB in both the nuclear and cytoplasmic
434 compartments compared to androgen-dependent prostate cancer cells. Consistent with UniProt
435 predicted isoforms, we report that NFIB also exists in multiple isoforms in prostate cancer cells,
436 with average molecular weights of 62 kDa, 57 kDa, 49 kDa, and 39 kDa.

437 Our observation of multiple NFIB isoforms is novel in prostate cancer cell lines, but has
438 been reported in other systems. The *NFIB* gene can undergo alternative splicing, giving rise to
439 nine variants[51], and the presence of multiple NFIB protein isoforms is consistent with reports from

440 UniProt[52], where NFIB has six reported isoforms (O00712 [NFIB_HUMAN], Entry version 172 [08
441 May 2019]). These isoforms have molecular weights of 47,442 Da (O00712-1), 22,251 Da
442 (O00712-2), 53,049 Da (O00712-4), 55,181 Da (O00712-5), and 33,525 Da (O00712-6). While
443 these do not match up exactly with our reported bands at 62 kDa, 57 kDa, 49 kDa, and 39 kDa,
444 NFIB a can undergo posttranslational modification like glycosylation[53] and sumoylation[54] which
445 could add to these molecular weights. *In vitro* translation assays have also identified NFI-B2 and
446 NFI-B3, at 47 kDa and 22 kDa, respectively[55], indicating that some of these splice variants are
447 expressed and functional. Significantly, the NFI-B3 isoform lacks the ability to bind DNA and
448 regulate gene expression and acts as a dominant negative factor in the presence of NFIB, NFIC,
449 and NFIX[55] Unfortunately, the NFIB antibody immunogen is a sequence shared by all but the
450 22,251 Da (O00712-2) isoform. Therefore, we do not know the status of this isoform in our
451 prostate cancer cell lines or prostate cancer tissues.

452 Although our previous studies showed that FOXA1 bridges the AR/NFIX interaction in
453 HeLa cells in Fluorescent Protein Förster Resonance Energy Transfer (FP-FRET) experiments[29],
454 we did observe some FRET signal between AR and NFIX, albeit this signal did not achieve
455 statistical significance. Our exogenous co-immunoprecipitation studies now demonstrate at least
456 one NFI, NFIB, is capable of interacting with the full length AR. What domains are responsible for
457 this interaction, whether this interaction occurs with AR splice variants, and what the functional
458 consequences of AR and NFIB interaction entail is under investigation.

459 In this present study, we investigated the role of NFIB in disease progression by using
460 LNCaP and their castration-resistant derivative cell line, C4-2B as a model of disease
461 progression. Over-expression of NFIB induced expression of PSA in LNCaP cells to levels
462 comparable with C4-2B cells. Our data supports that this is likely due to interactions with AR, as
463 we observed no increase in AR protein expression but instead noted increased AR activity in an
464 androgen-responsive promoter assay. Over-expression of NFIB also induced expression of other

465 secreted proteins and cytokines associated with and/or implicated in castration-resistant prostate
466 cancer, such as angiogenin[56], DDPIV (CD26)[57], IGFBP-2[58,59], and PSA[60].

467 These studies linking NFIB with more aggressive disease are more consistent with the
468 literature, wherein NFIB has been recently considered a proto-oncogene[61-66]. Our early studies
469 indicated that transient knockdown of *NFIB* increased the expression of AR-target genes[29,34], and
470 we believe this difference might be due to the adaptation that NFIB over-expression induces. For
471 example, in mouse models of lung cancer, Nfib increases chromatin accessibility[64], potentially
472 through interactions with FOXA1 we have demonstrated previously[29]. NFIB has also been
473 implicated in controlling components of the Polycomb Repressive Complex 2 (PRC2), which
474 includes EZH2 and EED. Over-expression of NFIB induces expression of EZH2 in melanoma[62]
475 and NFIB also interacts with EED[67].

476 Although our studies have focused on the role of NFIB in regulating AR expression and
477 activity, it is likely that NFIB also has roles independent of AR. For example, in mouse models of
478 small cell prostate cancer or lung cancer, Nfib is regularly amplified[68,69], and over-expression of
479 Nfib in a transgenic model of small cell lung cancer drives aggressive disease[63]. Our small cohort
480 of primary small cell prostate cancer samples strongly express NFIB. What the role for NFIB in
481 these AR-independent tumors also remains to be determined.

482 In summary, our study has described the expression of NFIB, AR, and synaptophysin in
483 a small cohort of prostate cancer patients. We report that NFIB is over-expressed in the nuclear
484 and cytoplasmic fractions of prostate cancer patient tissues and cell lines. We also report that
485 NFIB can interact with full length AR, and over-expression of NFIB can support increased
486 expression of canonical AR-target gene products, like PSA.

487

488 **Acknowledgements:**

489 We would like to thank the prostate cancer patients included in the tissue microarray for providing
490 their tissues and clinical data and Dr. Derek J. Taylor's laboratory for assisting with virus

generation. We would also like to thank Dr. Robert J. Matusik for his early support of these studies and critical feedback on the manuscript, and Daniel A. Barocas whose development of the Urologic Outcomes Database enabled linking outcomes data with this tissue microarray[35]. This work was supported in part by the Defense Health Program, through the Prostate Cancer Research Program Postdoctoral Training Award, under Award No. W81XWH-14-1-0312. Opinions, interpretations, conclusions and recommendations are those of the author and are not necessarily endorsed by the Department of Defense or U.S. Army. In the conduct of research utilizing recombinant DNA, the investigators adhered to NIH Guidelines for research involving recombinant DNA molecules. These studies were also supported in part by the National Cancer Institute of the National Institutes of Health under award number K99CA197315 and R00CA197315 (to MMG). The content is solely the responsibility of the authors and does not necessarily represent the official views of the National Institutes of Health.

Contributions:

JSN, PEC, GAG, and MMG designed the research studies. JSN, WNA, SEK, PP, and MMG conducted the experiments. JSN, WNA, SEK, and MMG acquired and analyzed data. JMMC and GAG performed pathological analysis of tumor sections. GAG provided the tissue microarray, which included clinical outcomes data whose collection was overseen by DAB and PEC for the Urologic Outcomes Database maintained at Vanderbilt University Medical Center. JM, GAG, and MMG wrote IRB protocols to acquire tissues and data. All authors contributed to writing the manuscript.

References:

1. Insitute, T. N. C. *PDQ Prostate Cancer Treatment*, <http://www.cancer.gov/cancertopics/pdq/treatment/prostate/HealthProfessional> (2014).
2. Salonen, A. J., Taari, K., Ala-Opas, M., Viitanen, J., Lundstedt, S. & Tammela, T. L. J. The FinnProstate Study VII: Intermittent Versus Continuous Androgen Deprivation in

519 Patients With Advanced Prostate Cancer. *The Journal of Urology* **187**, 2074-2081,
520 (2012).
521 3. Barrie SE, P. G., Goddard PM, Haynes BP, Dowsett M, Jarman M. Pharmacology of
522 novel steroidal inhibitors of cytochrome P450(17) alpha (17 alphahydroxylase/C17-20
523 lyase). *The Journal of Steroid Biochemistry and Molecular Biology* **50**, 267-273, (1994).
524 4. Tran, C., Ouk, S., Clegg, N. J., Chen, Y., Watson, P. A., Arora, V., Wongvipat, J., Smith-
525 Jones, P. M., Yoo, D., Kwon, A., Wasielewska, T., Welsbie, D., Chen, C., Higano, C. S.,
526 Beer, T. M., Hung, D. T., Scher, H. I., Jung, M. & Sawyers, C. L. Development of a
527 Second-Generation Antiandrogen for Treatment of Advanced Prostate Cancer. *Science*
528 *(New York, N.Y.)* **324**, 787-790, (2009).
529 5. Scher, H., Beer, T., Higano, C., Anand, A., Taplin, M., Efstathiou, E., Rathkopf, D.,
530 Shelkey, J., Yu, E., Alumkal, J., Hung, D., Hirmand, M., Seely, L., Morris, M., Danila, D.,
531 Humm, J., Larson, S., Fleisher, M. & Sawyers, C. - Antitumour activity of MDV3100 in
532 castration-resistant prostate cancer: a phase 1-2 study. *Lancet* **375**, 1437-1446, (2010).
533 6. Fizazi, K., Scher, H. I., Molina, A., Logothetis, C. J., Chi, K. N., Jones, R. J., Staffurth, J.
534 N., North, S., Vogelzang, N. J., Saad, F., Mainwaring, P., Harland, S., Goodman, O. B.,
535 Sternberg, C. N., Li, J. H., Kheoh, T., Haqq, C. M. & de Bono, J. S. Abiraterone acetate
536 for treatment of metastatic castration-resistant prostate cancer: final overall survival
537 analysis of the COU-AA-301 randomised, double-blind, placebo-controlled phase 3
538 study. *The Lancet Oncology* **13**, 983-992, (2012).
539 7. Bluemn, E. G., Coleman, I. M., Lucas, J. M., Coleman, R. T., Hernandez-Lopez, S.,
540 Tharakan, R., Bianchi-Frias, D., Dumpit, R. F., Kaipainen, A., Corella, A. N., Yang, Y. C.,
541 Nyquist, M. D., Mostaghel, E., Hsieh, A. C., Zhang, X., Corey, E., Brown, L. G., Nguyen,
542 H. M., Pienta, K., Ittmann, M., Schweizer, M., True, L. D., Wise, D., Rennie, P. S.,
543 Vessella, R. L., Morrissey, C. & Nelson, P. S. Androgen Receptor Pathway-Independent
544 Prostate Cancer Is Sustained through FGF Signaling. *Cancer Cell* **32**, 474-489.e476,
545 (2017).
546 8. Vis, A. N. & Schröder, F. H. Key targets of hormonal treatment of prostate cancer. Part
547 1: the androgen receptor and steroidogenic pathways. *BJU International* **104**, 438-448,
548 (2009).
549 9. Matei, D. V., Renne, G., Pimentel, M., Sandri, M. T., Zorzino, L., Botteri, E., De Cicco,
550 C., Musi, G., Brescia, A., Mazzoleni, F., Tringali, V., Detti, S. & de Cobelli, O.
551 Neuroendocrine Differentiation in Castration-Resistant Prostate Cancer: A Systematic
552 Diagnostic Attempt. *Clin.Genitourin.Cancer.*, (2012).
553 10. Beltran, H., Prandi, D., Mosquera, J. M., Benelli, M., Puca, L., Cyrta, J., Marotz, C.,
554 Giannopoulou, E., Chakravarthi, B. V. S. K., Varambally, S., Tomlins, S. A., Nanus, D.
555 M., Tagawa, S. T., Van Allen, E. M., Elemento, O., Sboner, A., Garraway, L. A., Rubin,
556 M. A. & Demichelis, F. Divergent clonal evolution of castration-resistant neuroendocrine
557 prostate cancer. *Nature Medicine* **22**, 298-305, (2016).
558 11. Aggarwal, R., Huang, J., Alumkal, J. J., Zhang, L., Feng, F. Y., Thomas, G. V.,
559 Weinstein, A. S., Friedl, V., Zhang, C., Witte, O. N., Lloyd, P., Gleave, M., Evans, C. P.,
560 Youngren, J., Beer, T. M., Rettig, M., Wong, C. K., True, L., Foye, A., Playdle, D., Ryan,
561 C. J., Lara, P., Chi, K. N., Uzunangelov, V., Sokolov, A., Newton, Y., Beltran, H.,
562 Demichelis, F., Rubin, M. A., Stuart, J. M. & Small, E. J. Clinical and Genomic
563 Characterization of Treatment-Emergent Small-Cell Neuroendocrine Prostate Cancer: A
564 Multi-institutional Prospective Study. *Journal of Clinical Oncology* **0**,
565 JCO.2017.2077.6880, (2018).
566 12. Aparicio, A., Logothetis, C. J. & Maity, S. N. Understanding the Lethal Variant of
567 Prostate Cancer: Power of Examining Extremes. *Cancer Discovery* **1**, 466-468, (2011).

13. Wang, W. & Epstein, J. I. Small Cell Carcinoma of the Prostate: A Morphologic and Immunohistochemical Study of 95 Cases. *American Journal of Surgical Pathology* **32**, 65-71, (2008).
14. Abrahamsson, P. A. Neuroendocrine differentiation in prostatic carcinoma. *Prostate* **39**, 135-148, (1999).
15. di Sant'Agnese, P. A. Neuroendocrine differentiation in human prostatic carcinoma. *Hum.Pathol.* **23**, 287-296, (1992).
16. Lin, D., Wyatt, A. W., Xue, H., Wang, Y., Dong, X., Haegert, A., Wu, R., Brahmbhatt, S., Mo, F., Jong, L., Bell, R. H., Anderson, S., Hurtado-Coll, A., Fazli, L., Sharma, M., Beltran, H., Rubin, M., Cox, M., Gout, P. W., Morris, J., Goldenberg, L., Volik, S. V., Gleave, M. E., Collins, C. C. & Wang, Y. High Fidelity Patient-Derived Xenografts for Accelerating Prostate Cancer Discovery and Drug Development. *Cancer Research* **74**, 1272-1283, (2014).
17. Terry, S. & Beltran, H. The many faces of neuroendocrine differentiation in prostate cancer progression. *Frontiers in Oncology* **4**, (2014).
18. Mosquera, J. M., Beltran, H., Park, K., MacDonald, T. Y., Robinson, B. D., Tagawa, S. T., Perner, S., Bismar, T. A., Erbersdobler, A., Dhir, R., Nelson, J. B., Nanus, D. M. & Rubin, M. A. Concurrent AURKA and MYCN gene amplifications are harbingers of lethal treatment-related neuroendocrine prostate cancer. *Neoplasia* **15**, 1-10, (2013).
19. Beltran, H., Tagawa, S. T., Park, K., MacDonald, T., Milowsky, M. I., Mosquera, J. M., Rubin, M. A. & Nanus, D. M. Challenges in Recognizing Treatment-Related Neuroendocrine Prostate Cancer. *Journal of Clinical Oncology* **30**, e386-e389, (2012).
20. Williamson, S. R., Zhang, S., Yao, J. L., Huang, J., Lopez-Beltran, A., Shen, S., Osunkoya, A. O., MacLennan, G. T., Montironi, R. & Cheng, L. ERG–TMPRSS2 rearrangement is shared by concurrent prostatic adenocarcinoma and prostatic small cell carcinoma and absent in small cell carcinoma of the urinary bladder: evidence supporting monoclonal origin. *Modern pathology : an official journal of the United States and Canadian Academy of Pathology, Inc* **24**, 1120-1127, (2011).
21. Beltran, H., Rickman, D. S., Park, K., Chae, S. S., Sboner, A., MacDonald, T. Y., Wang, Y., Sheikh, K. L., Terry, S. p., Tagawa, S. T., Dhir, R., Nelson, J. B., de la Taille, A., Allory, Y., Gerstein, M. B., Perner, S., Pienta, K. J., Chinnaiyan, A. M., Wang, Y., Collins, C. C., Gleave, M. E., Demichelis, F., Nanus, D. M. & Rubin, M. A. Molecular Characterization of Neuroendocrine Prostate Cancer and Identification of New Drug Targets. *Cancer Discovery* **1**, 487-495, (2011).
22. Lotan, T. L., Gupta, N. S., Wang, W., Toubaji, A., Haffner, M. C., Chaux, A., Hicks, J. L., Meeker, A. K., Bieberich, C. J., De Marzo, A. M., Epstein, J. I. & Netto, G. J. ERG gene rearrangements are common in prostatic small cell carcinomas. *Modern Pathology* **24**, 820-828, (2011).
23. Mertz, K. D., Setlur, S. R., Dhanasekaran, S. M., Demichelis, F., Perner, S., Tomlins, S., Tchinda, J., Laxman, B., Vessella, R. L., Beroukhimt, R., Lee, C., Chinnaiyan, A. M. & Rubin, M. A. Molecular Characterization of TMPRSS2-ERG Gene Fusion in the NCI-H660 Prostate Cancer Cell Line: A New Perspective for an Old Model. *Neoplasia* **9**, 200-IN203, (2007).
24. Palmgren, J. S., Karavadia, S. S. & Wakefield, M. R. Unusual and Underappreciated: Small Cell Carcinoma of the Prostate. *Seminars in Oncology* **34**, 22-29, (2007).
25. Jin, R. J., Wang, Y., Masumori, N., Ishii, K., Tsukamoto, T., Shappell, S. B., Hayward, S. W., Kasper, S. & Matusik, R. J. NE-10 Neuroendocrine Cancer Promotes the LNCaP Xenograft Growth in Castrated Mice. *Cancer Research* **64**, 5489-5495, (2004).
26. Gao, N., Zhang, J., Rao, M. A., Case, T. C., Mirosevich, J., Wang, Y., Jin, R., Gupta, A., Rennie, P. S. & Matusik, R. J. The role of hepatocyte nuclear factor-3 alpha (Forkhead

618 Box A1) and androgen receptor in transcriptional regulation of prostatic genes. *Molecular*
619 *Endocrinology* **17**, 1484-1507, (2003).
620 27. Gao, N., Ishii, K., Mirosevich, J., Kuwajima, S., Oppenheimer, S. R., Roberts, R. L.,
621 Jiang, M., Yu, X., Shappell, S. B., Caprioli, R. M., Stoffel, M., Hayward, S. W. & Matusik,
622 R. J. Forkhead box A1 regulates prostate ductal morphogenesis and promotes epithelial
623 cell maturation. *Development* **132**, 3431-3443, (2005).
624 28. DeGraff, D. J., Grabowska, M. M., Case, T. C., Yu, X., Herrick, M. K., Hayward, W. J.,
625 Strand, D. W., Cates, J. M., Hayward, S. W., Gao, N., Walter, M. A., Buttyan, R., Yi, Y.,
626 Kaestner, K. H. & Matusik, R. J. FOXA1 deletion in luminal epithelium causes prostatic
627 hyperplasia and alteration of differentiated phenotype. *Laboratory Investigation* **94**, 726-
628 739, (2014).
629 29. Grabowska, M. M., Elliott, A. D., DeGraff, D. J., Anderson, P. D., Anumanthan, G.,
630 Yamashita, H., Sun, Q., Friedman, D. B., Hachey, D. L., Yu, X., Sheehan, J. H., Ahn, J.-
631 M., Raj, G. V., Piston, D. W., Gronostajski, R. M. & Matusik, R. J. NFI Transcription
632 Factors Interact with FOXA1 to Regulate Prostate-Specific Gene Expression. *Molecular*
633 *Endocrinology* **28**, 949-964, (2014).
634 30. Zhang, J., Gao, N., DeGraff, D. J., Yu, X., Sun, Q., Case, T. C., Kasper, S. & Matusik, R.
635 J. Characterization of cis elements of the probasin promoter necessary for prostate-
636 specific gene expression. *The Prostate* **70**, 934-951, (2010).
637 31. Yeung, L. H., Read, J. T., Sorenson, P., Nelson, C. C., Jia, W. & Rennie, P. S.
638 Identification and characterization of a prostate-specific androgen-independent protein-
639 binding site in the probasin promoter. *Biochemical Journal* **371**, 843-855, (2003).
640 32. Jia, L., Berman, B. P., Jariwala, U., Yan, X., Cogan, J. P., Walters, A., Chen, T.,
641 Buchanan, G., Frenkel, B. & Coetzee, G. A. Genomic androgen receptor-occupied
642 regions with different functions, defined by histone acetylation, coregulators and
643 transcriptional capacity. *PLoS ONE* **3**, e3645, (2008). 2577007
644 33. Sharma, N. L., Massie, C. E., Ramos-Montoya, A., Zecchini, V., Scott, H. E., Lamb, A.
645 D., MacArthur, S., Stark, R., Warren, A. Y., Mills, I. G. & Neal, D. E. The androgen
646 receptor induces a distinct transcriptional program in castration-resistant prostate cancer
647 in man. *Cancer Cell* **23**, 35-47, (2013).
648 34. Grabowska, M. M., Kelly, S. M., Reese, A. L., Cates, J. M., Case, T. C., Zhang, J.,
649 DeGraff, D. J., Strand, D. W., Miller, N. L., Clark, P. E., Hayward, S. W., Gronostajski, R.
650 M., Anderson, P. D. & Matusik, R. J. Nfib regulates transcriptional networks that control
651 the development of prostatic hyperplasia. *Endocrinology* **157**, 1094-1109, (2016).
652 35. Goldstein, J., Borowsky, A. D., Goyal, R., Roland, J. T., Arnold, S. A., Gellert, L. L.,
653 Clark, P. E., Hameed, O. & Giannico, G. A. MAGI-2 in prostate cancer: an
654 immunohistochemical study. *Human Pathology* **52**, 83-91, (2016).
655 36. Mirosevich, J., Gao, N., Gupta, A., Shappell, S. B., Jove, R. & Matusik, R. J. Expression
656 and role of Foxa proteins in prostate cancer. *Prostate* **66**, 1013-1028, (2006).
657 37. Thalmann, G. N., Anezinis, P. E., Chang, S.-M., Zhau, H. E., Kim, E. E., Hopwood, V. L.,
658 Pathak, S., von Eschenbach, A. C. & Chung, L. W. K. Androgen-independent Cancer
659 Progression and Bone Metastasis in the LNCaP Model of Human Prostate Cancer.
660 *Cancer Research* **54**, 2577-2581, (1994).
661 38. Franco, O. E., Jiang, M., Strand, D. W., Peacock, J., Fernandez, S., Jackson, R. S., 2nd,
662 Revelo, M. P., Bhowmick, N. A. & Hayward, S. W. Altered TGF-β signaling in a
663 subpopulation of human stromal cells promotes prostatic carcinogenesis. *Cancer*
664 *Research* **71**, 1272-1281, (2011).
665 39. Jiang, M., Strand, D. W., Fernandez, S., He, Y., Yi, Y., Birbach, A., Qiu, Q., Schmid, J.,
666 Tang, D. G. & Hayward, S. W. Functional remodeling of benign human prostatic tissues
667 in vivo by spontaneously immortalized progenitor and intermediate cells. *Stem cells*
668 *(Dayton, Ohio)* **28**, 344-356, (2010).

669 40. Dehm, S. M., Schmidt, L. J., Heemers, H. V., Vessella, R. L. & Tindall, D. J. Splicing of a
670 Novel Androgen Receptor Exon Generates a Constitutively Active Androgen
671 Receptor that Mediates Prostate Cancer Therapy Resistance. *Cancer Research* **68**,
672 5469-5477, (2008).
673 41. Morgenstern, J. P. & Land, H. Advanced mammalian gene transfer: high titre retroviral
674 vectors with multiple drug selection markers and a complementary helper-free packaging
675 cell line. *Nucleic Acids Research* **18**, 3587-3596, (1990).
676 42. Stewart, S. A., Dykxhoorn, D. M., Palliser, D., Mizuno, H., Yu, E. Y., An, D. S., Sabatini,
677 D. M., Chen, I. S. Y., Hahn, W. C., Sharp, P. A., Weinberg, R. A. & Novina, C. D.
678 Lentivirus-delivered stable gene silencing by RNAi in primary cells. *RNA (New York,*
679 *N.Y.)* **9**, 493-501, (2003).
680 43. Schneider, C. A., Rasband, W. S. & Eliceiri, K. W. NIH Image to ImageJ: 25 years of
681 image analysis. *Nature Methods* **9**, 671, (2012).
682 44. Abramoff, M. D., Magalhaes, P. J. & Ram, S. J. Image Processing with ImageJ.
683 *Biophotonics International* **11**, 36-42, (2004).
684 45. Image J (U. S. National Institutes of Health, Bethesda, Maryland, USA).
685 46. Ling, G., Hauer, C. R., Gronostajski, R. M., Pentecost, B. T. & Ding, X. Transcriptional
686 Regulation of Rat CYP2A3 by Nuclear Factor 1: IDENTIFICATION OF A NOVEL NFI-A
687 ISOFORM, AND EVIDENCE FOR TISSUE-SELECTIVE INTERACTION OF NFI WITH
688 THE CYP2A3 PROMOTER IN VIVO. *Journal of Biological Chemistry* **279**, 27888-27895,
689 (2004).
690 47. Delk, N. A. & Farach-Carson, M. C. Interleukin-6: A bone marrow stromal cell paracrine
691 signal that induces neuroendocrine differentiation and modulates autophagy in bone
692 metastatic PCa cells. *Autophagy* **8**, 650-663, (2012).
693 48. Nakashima, J., Tachibana, M., Horiguchi, Y., Oya, M., Ohigashi, T., Asakura, H. &
694 Murai, M. Serum Interleukin 6 as a Prognostic Factor in Patients with Prostate Cancer.
695 *Clinical Cancer Research* **6**, 2702-2706, (2000).
696 49. Adler, H. L., McCurdy, M. A., Kattan, M. W., Timme, T. L., Scardino, P. T. & Thompson,
697 T. C. ELEVATED LEVELS OF CIRCULATING INTERLEUKIN-6 AND TRANSFORMING
698 GROWTH FACTOR-beta 1 IN PATIENTS WITH METASTATIC PROSTATIC
699 CARCINOMA. *The Journal of Urology* **161**, 182-187, (1999).
700 50. Twillie, D. A., Eisenberger, M. A., Carducci, M. A., Hseih, W.-S., Kim, W. Y. & Simons, J.
701 W. Interleukin-6: A candidate mediator of human prostate cancer morbidity. *Urology* **45**,
702 542-549, (1995).
703 51. Chen, K.-S., Lim, J. W. C., Richards, L. J. & Bunt, J. The convergent roles of the nuclear
704 factor I transcription factors in development and cancer. *Cancer Letters* **410**, 124-138,
705 (2017).
706 52. Consortium, T. U. UniProt: a worldwide hub of protein knowledge. *Nucleic Acids*
707 *Research* **47**, D506-D515, (2018).
708 53. Mukhopadhyay, S. S. & Rosen, J. M. The C-terminal domain of the nuclear factor I-B2
709 isoform is glycosylated and transactivates the WAP gene in the JEG-3 cells. *Biochemical*
710 *and Biophysical Research Communications* **358**, 770-776, (2007).
711 54. Yang, S. H., Galanis, A., Witty, J. & Sharrocks, A. D. An extended consensus motif
712 enhances the specificity of substrate modification by SUMO. *The EMBO Journal* **25**,
713 5083-5093, (2006).
714 55. Liu, Y., Bernard, H.-U. & Apt, D. NFI-B3, a Novel Transcriptional Repressor of the
715 Nuclear Factor I Family, Is Generated by Alternative RNA Processing. *Journal of*
716 *Biological Chemistry* **272**, 10739-10745, (1997).
717 56. Li, S., Hu, M. G., Sun, Y., Yoshioka, N., Ibaragi, S., Sheng, J., Sun, G., Kishimoto, K. &
718 Hu, G.-F. Angiogenin mediates androgen-stimulated prostate cancer growth and
719 enables castration resistance. *Molecular cancer research : MCR* **11**, 1203-1214, (2013).

720 57. Park, J. W., Lee, J. K., Witte, O. N. & Huang, J. FOXA2 is a sensitive and specific
721 marker for small cell neuroendocrine carcinoma of the prostate. *Modern Pathology*,
722 (2017).
723 58. Degraff, D. J., Aguiar, A. A. & Sikes, R. A. Disease evidence for IGFBP-2 as a key
724 player in prostate cancer progression and development of osteosclerotic lesions.
725 *American Journal of Translational Research* **1**, 115-130, (2009).
726 59. Kiyama, S., Morrison, K., Zellweger, T., Akbari, M., Cox, M., Yu, D., Miyake, H. &
727 Gleave, M. E. Castration-Induced Increases in Insulin-Like Growth Factor-Binding
728 Protein 2 Promotes Proliferation of Androgen-independent Human Prostate LNCaP
729 Tumors. *Cancer Research* **63**, 3575-3584, (2003).
730 60. Moreira, D. M., Howard, L. E., Sourbeer, K. N., Amarasekara, H. S., Chow, L. C.,
731 Cockrell, D. C., Hanyok, B. T., Aronson, W. J., Kane, C. J., Terris, M. K., Amling, C. L.,
732 Cooperberg, M. R., Liede, A. & Freedland, S. J. Predictors of Time to Metastasis in
733 Castration-resistant Prostate Cancer. *Urology* **96**, 171-176, (2016).
734 61. Wu, Y., Zhang, J., Hou, S., Cheng, Z. & Yuan, M. Non-small cell lung cancer: miR-30d
735 suppresses tumor invasion and migration by directly targeting NFIB. *Biotechnology*
736 *Letters* **39**, 1827-1834, (2017).
737 62. Fane, M. E., Chhabra, Y., Hollingsworth, D. E. J., Simmons, J. L., Spoerri, L., Oh, T. G.,
738 Chauhan, J., Chin, T., Harris, L., Harvey, T. J., Muscat, G. E. O., Goding, C. R., Sturm,
739 R. A., Haass, N. K., Boyle, G. M., Piper, M. & Smith, A. G. NFIB Mediates BRN2 Driven
740 Melanoma Cell Migration and Invasion Through Regulation of EZH2 and MITF.
741 *EBioMedicine* **16**, 63-75, (2017).
742 63. Wu, N., Jia, D., Ibrahim, A. H., Bachurski, C. J., Gronostajski, R. M. & MacPherson, D.
743 NFIB overexpression cooperates with Rb/p53 deletion to promote small cell lung cancer.
744 *Oncotarget* **7**, 57514-57524, (2016).
745 64. Denny, S. K., Yang, D., Chuang, C.-H., Brady, J. J., Lim, J. S., Grüner, B. M., Chiou, S.-
746 H., Schep, A. N., Baral, J., Hamard, C., Antoine, M., Wislez, M., Kong, C. S., Connolly,
747 A. J., Park, K.-S., Sage, J., Greenleaf, W. J. & Winslow, M. M. Nfib Promotes Metastasis
748 through a Widespread Increase in Chromatin Accessibility. *Cell* **166**, 328-342, (2016).
749 65. Semenova, Ekaterina A., Kwon, M.-c., Monkhorst, K., Song, J.-Y., Bhaskaran, R.,
750 Krijgsman, O., Kuilman, T., Peters, D., Buikhuisen, Wieneke A., Smit, Egbert F.,
751 Pritchard, C., Cozijnsen, M., van der Vliet, J., Zevenhoven, J., Lambooij, J.-P., Proost,
752 N., van Montfort, E., Velds, A., Huijbers, Ivo J. & Berns, A. Transcription Factor NFIB Is
753 a Driver of Small Cell Lung Cancer Progression in Mice and Marks Metastatic Disease in
754 Patients. *Cell Reports* **16**, 631-643, (2016).
755 66. Becker-Santos, D. D., Thu, K. L., English, J. C., Pikor, L. A., Martinez, V. D., Zhang, M.,
756 Vucic, E. A., Luk, M. T. Y., Carraro, A., Korbelik, J., Piga, D., Lhomme, N. M., Tsay, M.
757 J., Yee, J., MacAulay, C. E., Lam, S., Lockwood, W. W., Robinson, W. P., Jurisica, I. &
758 Lam, W. L. Developmental transcription factor NFIB is a putative target of oncofetal
759 miRNAs and is associated with tumour aggressiveness in lung adenocarcinoma. *The*
760 *Journal of Pathology* **240**, 161-172, (2016).
761 67. Cao, Q., Wang, X., Zhao, M., Yang, R., Malik, R., Qiao, Y., Poliakov, A., Yocum, A. K.,
762 Li, Y., Chen, W., Cao, X., Jiang, X., Dahiya, A., Harris, C., Feng, F. Y., Kalantry, S., Qin,
763 Z. S., Dhanasekaran, S. M. & Chinnaiyan, A. M. The Central Role of EED in the
764 Orchestration of Polycomb Group Complexes. *Nature Communications* **5**, 3127-3127,
765 (2014).
766 68. Dooley, A. L., Winslow, M. M., Chiang, D. Y., Banerji, S., Stransky, N., Dayton, T. L.,
767 Snyder, E. L., Senna, S., Whittaker, C. A., Bronson, R. T., Crowley, D., Barretina, J.,
768 Garraway, L., Meyerson, M. & Jacks, T. Nuclear factor I/B is an oncogene in small cell
769 lung cancer. *Genes & Development* **25**, 1470-1475, (2011).

770 69. Zhou, Z., Flesken-Nikitin, A., Corney, D. C., Wang, W., Goodrich, D. W., Roy-Burman, P.
771 & Nikitin, A. Y. Synergy of p53 and Rb Deficiency in a Conditional Mouse Model for
772 Metastatic Prostate Cancer. *Cancer Research* **66**, 7889-7898, (2006).

773

774

775 **Figure Legends**

776 **Figure 1: Expression of AR, synaptophysin, and NFIB in human prostate.** Representative
777 images from the human tissue microarray, representing normal prostate, prostate cancer, and
778 castration-resistant prostate cancer. H&E: Hematoxylin and eosin; SYP: synaptophysin

779

780 **Figure 2: Expression of NFIB, AR, and synaptophysin in prostate and primary prostate**
781 **cancer.** Expression of NFIB (**A**), AR (**B**), and synaptophysin (**C**) in the nuclear and cytoplasmic
782 fractions of normal prostate and prostate cancer. Intensity and distribution scores in the nuclear
783 and cytoplasmic compartments of each core were added together to generate a composite
784 expression score for each protein of interest and patient averages were generated. Data were
785 analyzed using the Wilcoxon matched-pairs signed rank test. For analysis of association of
786 Gleason score with NFIB (**D**), AR (**E**), and synaptophysin (**F**) staining, unique core values were
787 used. Significant values are reported relative to Gleason score 3. Data were analyzed using the
788 Kruskal-Wallis test with Dunn's multiple comparisons test. SYP: synaptophysin * $P < 0.05$; **** $P<$
789 0.0001

790

791 **Figure 3: Cox regression of NFIB expression in prostate cancer. A**. Case processing
792 summary of NFIB as a single variable to predict time to biochemical recurrence (event) in days.
793 **B/C.** Nuclear and cytoplasmic NFIB alone do not predict biochemical recurrence. Variables in the
794 Cox regression model. **D**. Case processing summary of cytoplasmic-to-nuclear NFIB ratio and
795 surgical margin status to predict time to biochemical recurrence in days. **E.** Cox regression model
796 predicting time to biochemical recurrence using the cytoplasmic-to-nuclear NFIB ratio. **F.** Cox
797 regression model including positive margin status and nuclear-to-cytoplasmic NFIB ratio. B:
798 unstandardized regression coefficient; SE: standard error; Exp (B): hazard ratio; CI: confidence
799 interval; df: degrees of freedom

800

801 **Figure 4: NFIB, AR, and synaptophysin expression in primary and castration-resistant**
802 **prostate cancer.** Expression of NFIB (**A**), AR (**B**), and synaptophysin (**C**) in the nuclear and
803 cytoplasmic fractions of human prostatic tissues. Intensity and distribution scores in the nuclear
804 and cytoplasmic compartments of each core were added together to generate a composite
805 expression score for each protein of interest. An average value was generated for each patient.
806 Significant values are reported between prostate cancer and normal prostate or castration-
807 resistant prostate cancer. Data were analyzed using the Kruskal-Wallis test with Dunn's multiple
808 comparisons test. PCa: prostate cancer; CRPCa: castration-resistant prostate cancer; SYP:
809 synaptophysin ** P< 0.01; *** P< 0.001; **** P< 0.0001
810
811 **Figure 5: NFIB is expressed in prostate cancer cell lines and interacts with AR. A.** NFIB
812 expression in prostate cancer cell lines. Expression of NFIB in NFIB-low JEG-3 cells, androgen-
813 dependent (LNCaP), castration-resistant (C4-2B, 22RV1), and androgen independent (PC3, DU-
814 145) prostate cancer cells. **B.** Nuclear and cytoplasmic localization of NFIB. Nuclear and
815 cytoplasmic preparations of LNCaP, C4-2B, and 22RV1 cells, analyzed for AR and NFIB
816 expression. Nuclear loading control: Lamin B1; cytoplasmic loading control: GAPDH; N: nuclear;
817 C: cytoplasmic **C.** NFIB interacts with AR. Transient transfection of JEG-3 cells with Vector, NFIB,
818 full length AR (AR-FL), or AR-FL and NFIB, followed by co-immunoprecipitation with an antibody
819 against NFIB and Western blotting for AR and NFIB. **D.** Generation of 3X-FLAG-NFIB cells.
820 Western blot analysis of Flag expression in vector and 3X-FLAG-NFIB LNCaP and C4-2B cells.
821 Star: antibody heavy chain IgG. IP: immunoprecipitation
822
823 **Figure 6: NFIB supports PSA expression. A.** Human cytokine arrays exposed to lysates from
824 LNCaP and C4-2B cells expressing the vector or 3X-FLAG-NFIB construct. Dashed box denotes
825 location of DPPIV dots, solid box with tick marks outlines PSA dots. Double dots in upper left,
826 right, and lower left are positive controls. Lower right hand corner is empty and a negative control.

827 **B.** Quantification of integrated density for proteome arrays from A, adjusted for background and
828 normalized respective vector positive controls. **C.** Comparison of cytokine secretion across cell
829 lines, presented as cytokine integrated density divided by average positive control integrated
830 density of each cell line. **D.** Prostate specific antigen enhancer-promoter (PSA-EP) luciferase
831 activity in vector and 3X-FLAG-NFIB over-expressing cells. Data presented as fold change PSA-
832 EP-luciferase over SV40-renilla, normalized to vector. Data were analyzed using the Mann-
833 Whitney U test. **E.** Prostate specific antigen enhancer promoter (PSA-EP) luciferase activity in
834 vector and NFIB over-expressing cells. Data presented as fold change PSA-EP-luciferase over
835 SV40-renilla, normalized to LNCaP vector expression. Data were analyzed using the Mann-
836 Whitney U test, comparing vector to NFIB luciferase changes by cell line. ** $P < 0.01$
837
838 **Supplemental Figure 1: Expression of AR, synaptophysin, and NFIB in human prostate. A.**
839 Representative images from the human tissue microarray, representing normal prostate, prostate
840 cancer, and castration-resistant prostate cancer. **B.** FOXA1 and NFIB straining in primary human
841 small cell prostate cancer. H&E: Hematoxylin and eosin; SYP: synaptophysin
842
843 **Supplemental Figure 2: Correlations between NFIB, AR, and synaptophysin in prostate**
844 **cancer.** Spearman correlations between nuclear and cytoplasmic staining for NFIB, AR, and
845 synaptophysin in primary prostate cancer (**A**), both primary and castration-resistant prostate
846 cancer (**B**), and castration-resistant only (**C**).
847
848 **Supplemental Figure 3: Expression of NFIB, AR, and synaptophysin across prostate**
849 **diseases. A.** Cytoplasmic-to-nuclear ratio of NFIB does not vary by Gleason pattern by core or
850 by patient tumor stage. **B/C/D.** Expression of NFIB (**B**), AR (**C**), and synaptophysin (**D**) in the
851 nuclear and cytoplasmic fractions of human prostatic tissues. Intensity and distribution scores in
852 the nuclear and cytoplasmic compartments of each core were added together to generate a

853 composite expression score for each protein of interest. Data were analyzed using the Kruskal-
854 Wallis test with Dunn's multiple comparisons test. Significant values are reported between normal
855 prostate (normal) and diseased prostate. BPH: benign prostatic hyperplasia; HGPIN: high grade
856 prostatic intraepithelial neoplasia; Adj. Normal: adjacent normal; PCa: prostate cancer; CRPCa:
857 castration-resistant prostate cancer; SYP: synaptophysin * $P < 0.05$; ** $P< 0.01$; *** $P< 0.001$; ****
858 $P< 0.0001$
859
860 **Supplemental Figure 4: NFIB isoforms. A.** Expression of NFIB in stromal and epithelial cells
861 derived from BPH patients (BHPrS-1, BHPrE-1) and non-hyperplastic prostate epithelial cells
862 (NHPrE-1). Cancer cell lines shown as control. **B.** Calculated molecular weights of NFIB. **C.** NFIB
863 exists in several isoforms in PC-3 cells. Transient over-expression of vector or NFIB or knockdown
864 of non-targeting siRNA or NFIB in PC-3 cells. **D.** NFIB exists in several isoforms. Transient
865 knockdown of non-targeting siRNA or NFIB in JEG-3, LNCaP, C4-2B, and 22RV1 cells.
866

Figure 1

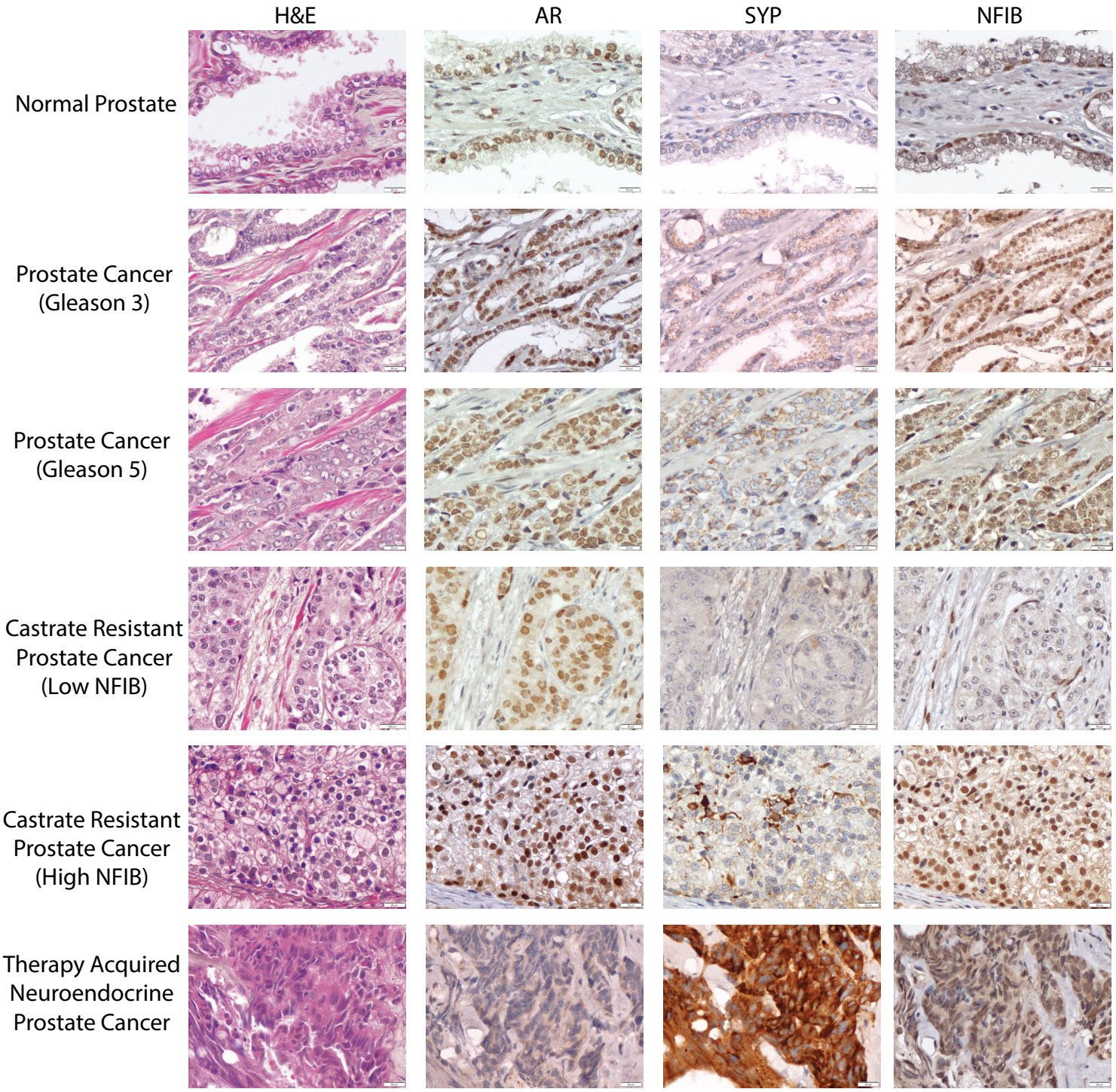
H&E
AR
SYP
NFIB
Normal Prostate
Prostate Cancer (Gleason 3)
Prostate Cancer (Gleason 5)
Castrate Resistant Prostate Cancer (Low NFIB)
Castrate Resistant Prostate Cancer (High NFIB)
Therapy Acquired Neuroendocrine Prostate Cancer

Figure 2

A.

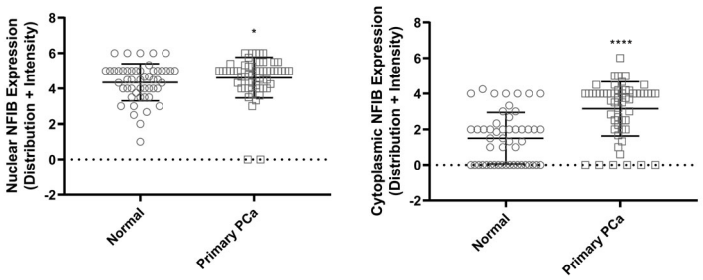

B.

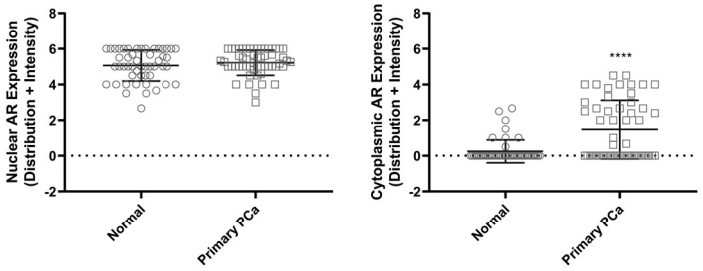

C.

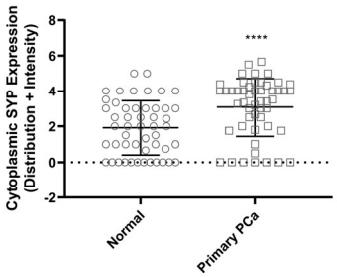

D.

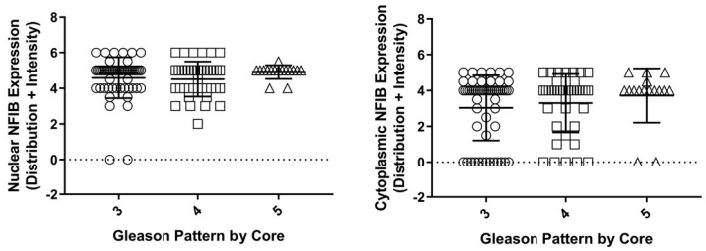

E.

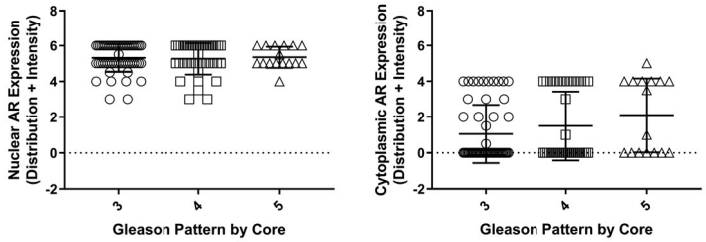

F.

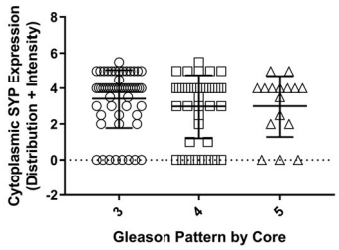

Figure 3

A.

Case Processing Summary

		N	Percent
Cases available in analysis	Event[a]	32	57.1%
	Censored	19	33.9%
	Total	51	91.1%
Cases dropped	Cases with missing values	5	8.9%
	Cases with negative time	0	0.0%
	Censored cases before the earliest event in a stratum	0	0.0%
	Total	5	8.9%
Total		56	100.0%

a. Dependent Variable: biochemical_recur_days

B.

Variables in the Equation

	B	SE	Wald	df	Sig.	Exp(B)	95.0% CI for Exp(B) Lower	Upper
Nuclear NFIB expression	-0.034	0.148	0.052	1	0.820	0.967	0.723	1.292

C.

Variables in the Equation

	B	SE	Wald	df	Sig.	Exp(B)	95.0% CI for Exp(B) Lower	Upper
Cytoplasmic NFIB expression	0.140	0.110	1.616	1	0.204	1.150	0.927	1.427

D.

Case Processing Summary

		N	Percent
Cases available in analysis	Event[a]	31	55.4%
	Censored	18	32.1%
	Total	49	87.5%
Cases dropped	Cases with missing values	7	12.5%
	Cases with negative time	0	0.0%
	Censored cases before the earliest event in a stratum	0	0.0%
	Total	7	12.5%
Total		56	100.0%

a. Dependent Variable: biochemical_recur_days

E.

Variables in the Equation

	B	SE	Wald	df	Sig.	Exp(B)	95.0% CI for Exp(B) Lower	Upper
NFIB Cytoplasmic to Nuclear Ratio	1.052	0.554	3.603	1	0.058	2.864	0.966	8.491

F.

Variables in the Equation

	B	SE	Wald	df	Sig.	Exp(B)	95.0% CI for Exp(B) Lower	Upper
NFIB Cytoplasmic to Nuclear Ratio	2.189	0.766	8.166	1	0.004	8.930	1.989	40.086
Positive Margin Status	2.084	0.469	19.757	1	0.00001	8.035	3.206	20.138

Figure 4

A.

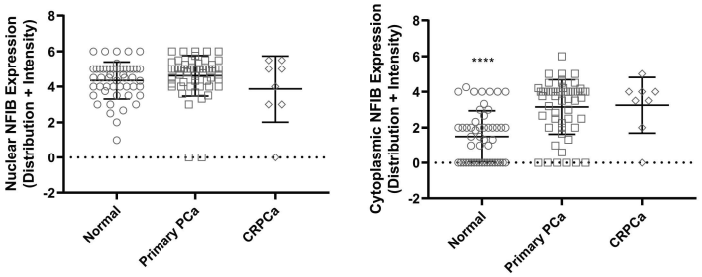
Nuclear NFIB Expression
(Distribution + Intensity)
Normal
Primary PCa
CRPCa
Cytoplasmic NFIB Expression
(Distribution + Intensity)
****

B.

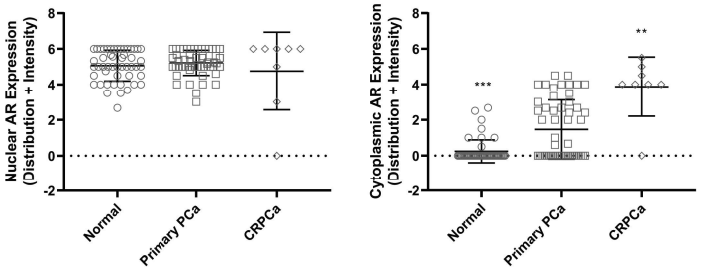
Nuclear AR Expression
(Distribution + Intensity)
Normal
Primary PCa
CRPCa
Cytoplasmic AR Expression
(Distribution + Intensity)
***
**

C.

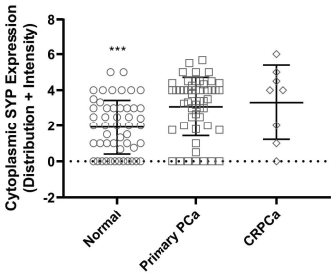
Cytoplasmic SYP Expression
(Distribution + Intensity)
***
Normal
Primary PCa
CRPCa

Figure 5

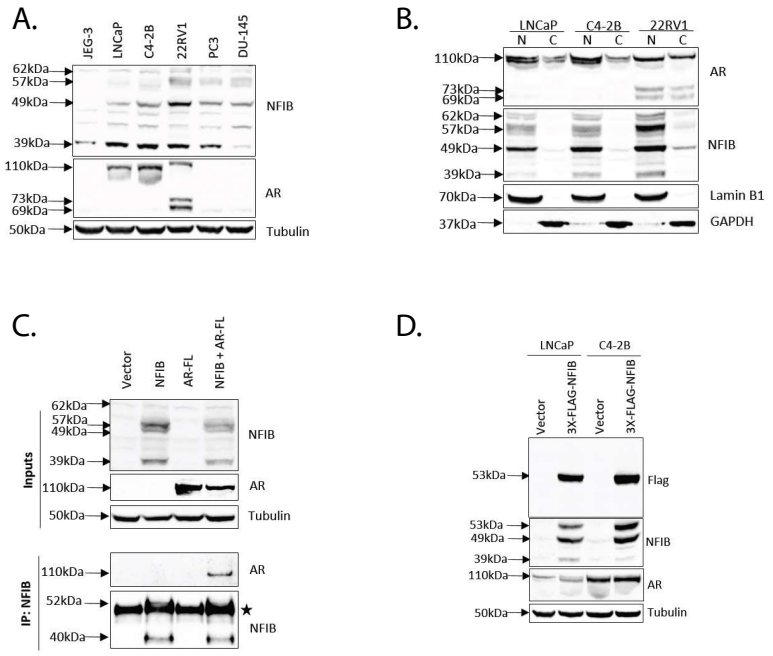
A.
JEG-3
LNCaP
C4-2B
22RV1
PC3
DU-145
62kDa
57kDa
49kDa
39kDa
NFIB
110kDa
73kDa
69kDa
AR
50kDa
Tubulin
B.
LNCaP
C4-2B
22RV1
N
C
110kDa
AR
73kDa
69kDa
62kDa
57kDa
49kDa
39kDa
NFIB
70kDa
Lamin B1
37kDa
GAPDH
C.
Vector
NFIB
AR-FL
NFIB + AR-FL
Inputs
62kDa
57kDa
49kDa
39kDa
NFIB
110kDa
AR
50kDa
Tubulin
IP: NFIB
110kDa
AR
52kDa
★
40kDa
NFIB
D.
LNCaP
C4-2B
Vector
3X-FLAG-NFIB
53kDa
Flag
53kDa
49kDa
39kDa
NFIB
110kDa
AR
50kDa
Tubulin

Figure 6

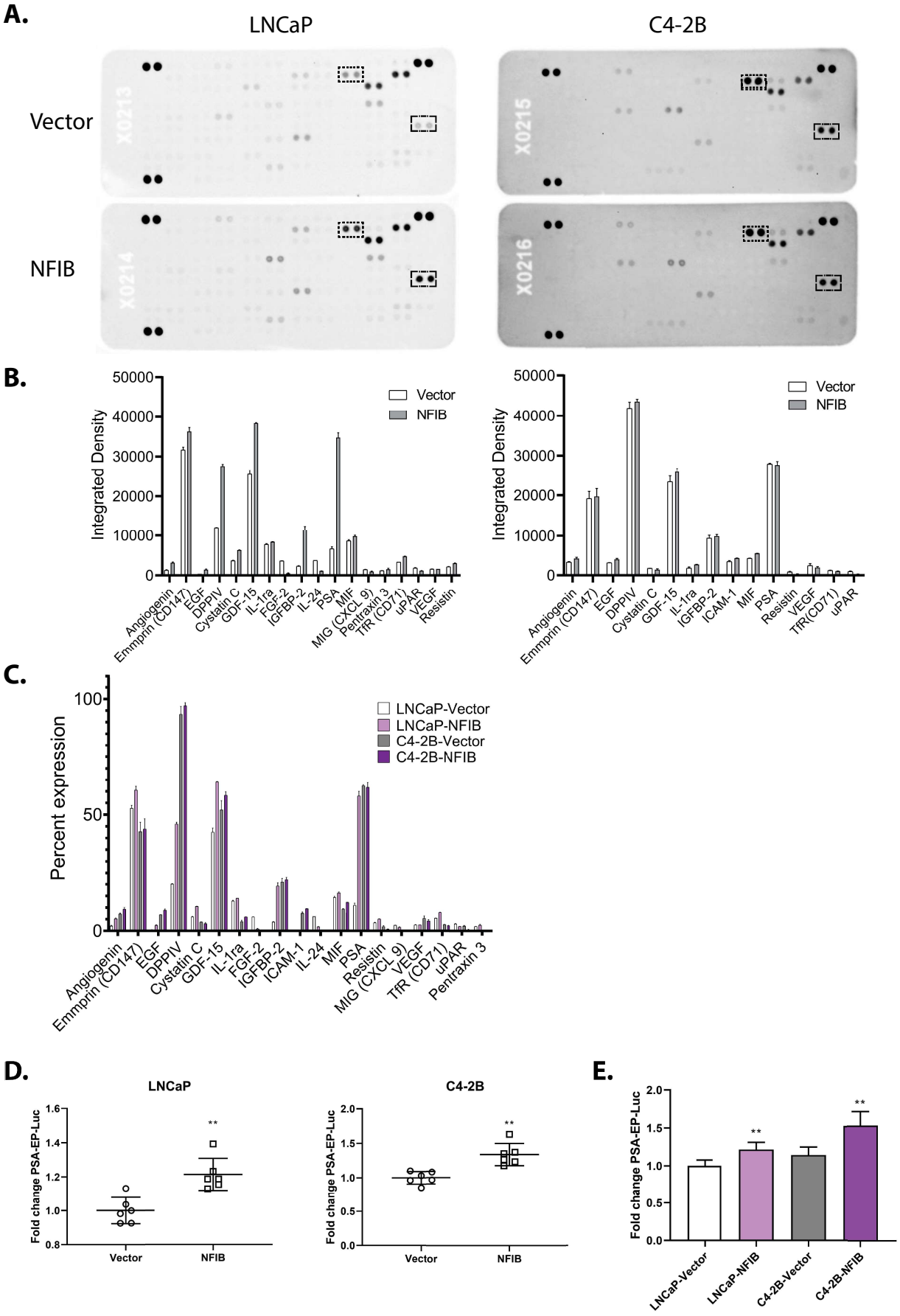
A.
LNCaP
C4-2B
Vector
NFIB
X0213
X0214
X0215
X0216
B.
Integrated Density
Vector
NFIB
Angiogenin
Emmprin (CD147)
EGF
DPPIV
Cystatin C
GDF-15
IL-1ra
FGF-2
IGFBP-2
IL-24
PSA
MIF
MIG (CXCL 9)
Pentraxin 3
TfR (CD71)
uPAR
VEGF
Resistin
ICAM-1
TfR(CD71)
C.
Percent expression
LNCaP-Vector
LNCaP-NFIB
C4-2B-Vector
C4-2B-NFIB
D.
LNCaP
C4-2B
Fold change PSA-EP-Luc
Vector
NFIB
E.
Fold change PSA-EP-Luc
LNCaP-Vector
LNCaP-NFIB
C4-2B-Vector
C4-2B-NFIB

Supp 1

A.

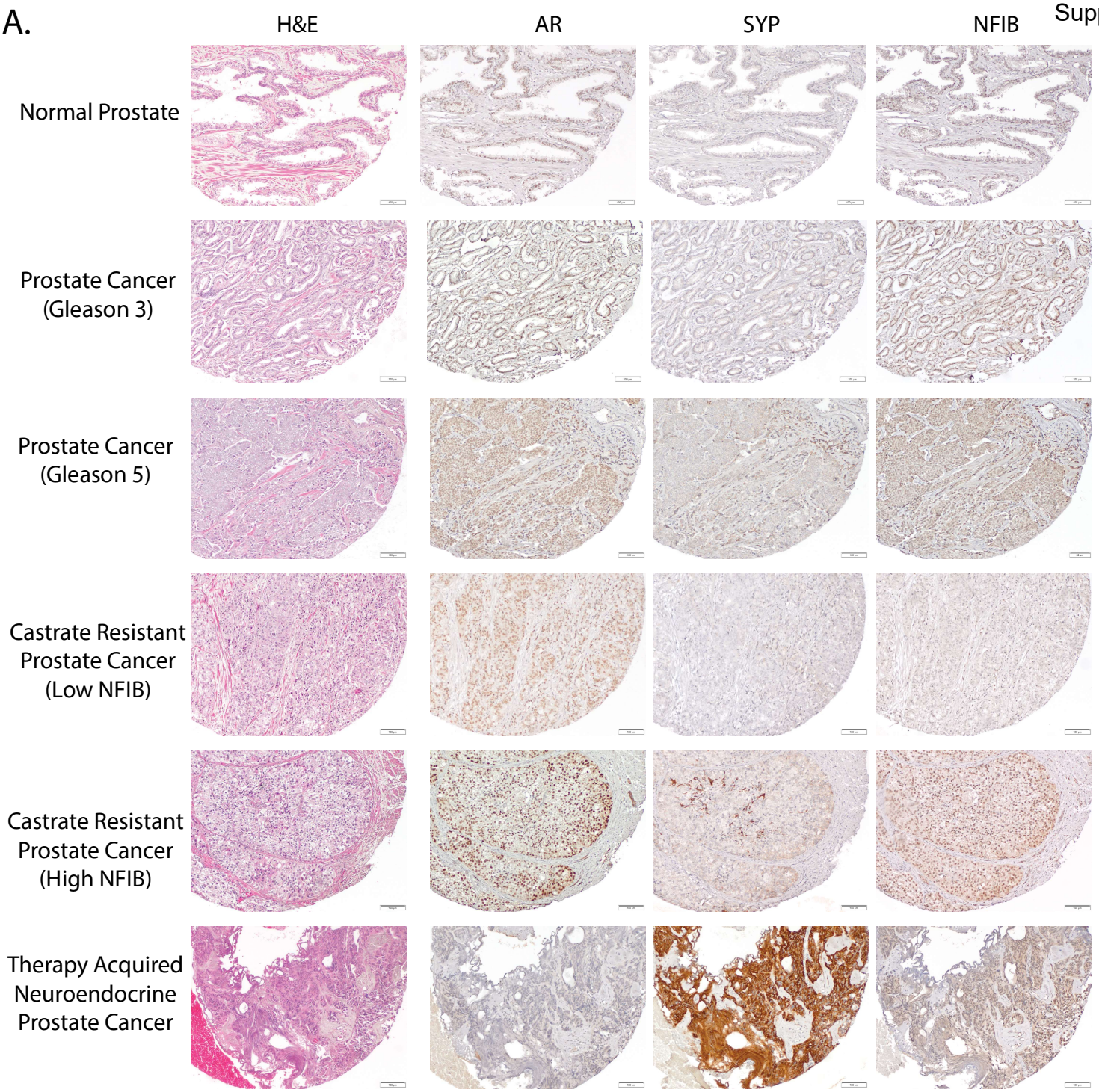
H&E
AR
SYP
NFIB
Normal Prostate
Prostate Cancer (Gleason 3)
Prostate Cancer (Gleason 5)
Castrate Resistant Prostate Cancer (Low NFIB)
Castrate Resistant Prostate Cancer (High NFIB)
Therapy Acquired Neuroendocrine Prostate Cancer

B.

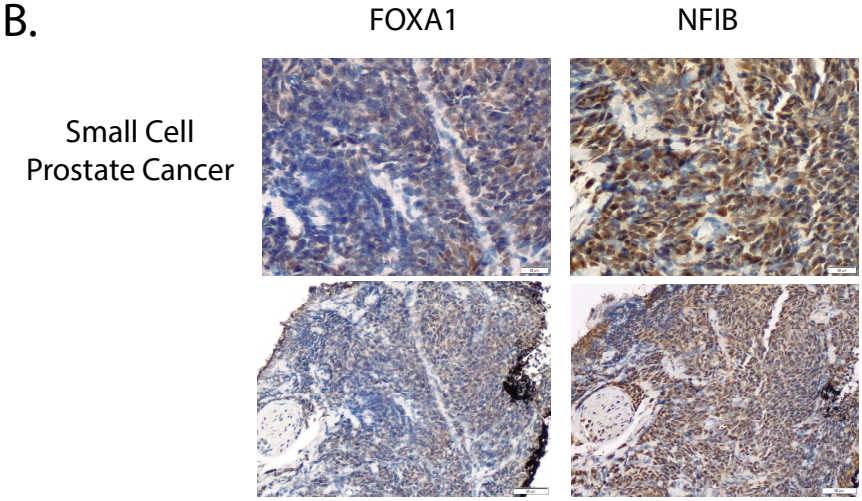
FOXA1
NFIB
Small Cell Prostate Cancer

A.

Correlations

			NFIB_Tumor_Nuclear	NFIB_Tumor_Cytoplasmic	AR_Tumor_Nuclear	AR_Tumor_Cytoplasmic	SYP_Tumor_Cytoplasmic
Spearman's rho	NFIB_Tumor_Nuclear	Correlation Coefficient	1.000	.305**	.419**	0.085	0.111
		Sig. (2-tailed)		0.001	1.875E-06	0.359	0.228
		N	120	120	120	120	120
	NFIB_Tumor_Cytoplasmic	Correlation Coefficient	.305**	1.000	.248**	.447**	.464**
		Sig. (2-tailed)	0.001		0.006	3.135E-07	9.483E-08
		N	120	120	120	120	120
	AR_Tumor_Nuclear	Correlation Coefficient	.419**	.248**	1.000	0.109	.350**
		Sig. (2-tailed)	1.875E-06	0.006		0.234	0.000
		N	120	120	120	120	120
	AR_Tumor_Cytoplasmic	Correlation Coefficient	0.085	.447**	0.109	1.000	.487**
		Sig. (2-tailed)	0.359	3.135E-07	0.234		1.638E-08
		N	120	120	120	120	120
	SYP_Tumor_Cytoplasmic	Correlation Coefficient	0.111	.464**	.350**	.487**	1.000
		Sig. (2-tailed)	0.228	9.483E-08	9.050E-05	1.638E-08	
		N	120	120	120	120	120

**. Correlation is significant at the 0.01 level (2-tailed).

B.

Correlations

			NFIB_Tumor_Nuclear	NFIB_Tumor_Cytoplasmic	AR_Tumor_Nuclear	AR_Tumor_Cytoplasmic	SYP_Tumor_Cytoplasmic
Spearman's rho	NFIB_Tumor_Nuclear	Correlation Coefficient	1.000	.321**	.394**	0.061	0.123
		Sig. (2-tailed)		2.176E-04	4.151E-06	0.494	0.168
		N	128	128	128	128	128
	NFIB_Tumor_Cytoplasmic	Correlation Coefficient	.321**	1.000	.228**	.381**	.473**
		Sig. (2-tailed)	2.176E-04		0.010	9.192E-06	1.766E-08
		N	128	128	128	128	128
	AR_Tumor_Nuclear	Correlation Coefficient	.394**	.228**	1.000	0.152	.279**
		Sig. (2-tailed)	4.151E-06	0.010		0.088	0.001
		N	128	128	128	128	128
	AR_Tumor_Cytoplasmic	Correlation Coefficient	0.061	.381**	0.152	1.000	.419**
		Sig. (2-tailed)	0.494	0.000	0.088		8.711E-07
		N	128	128	128	128	128
	SYP_Tumor_Cytoplasmic	Correlation Coefficient	0.123	.473**	.279**	.419**	1.000
		Sig. (2-tailed)	0.168	0.000	0.001	8.711E-07	
		N	128	128	128	128	128

**. Correlation is significant at the 0.01 level (2-tailed).

C.

Correlations

			NFIB_Tumor_Nuclear	NFIB_Tumor_Cytoplasmic	AR_Tumor_Nuclear	AR_Tumor_Cytoplasmic	SYP_Tumor_Cytoplasmic
Spearman's rho	NFIB_Tumor_Nuclear	Correlation Coefficient	1.000	0.625	0.250	-0.058	0.317
		Sig. (2-tailed)		0.098	0.550	0.891	0.444
		N	8	8	8	8	8
	NFIB_Tumor_Cytoplasmic	Correlation Coefficient	0.625	1.000	-0.084	-0.320	.735*
		Sig. (2-tailed)	0.098		0.843	0.439	0.038
		N	8	8	8	8	8
	AR_Tumor_Nuclear	Correlation Coefficient	0.250	-0.084	1.000	.712*	-0.466
		Sig. (2-tailed)	0.550	0.843		0.048	0.244
		N	8	8	8	8	8
	AR_Tumor_Cytoplasmic	Correlation Coefficient	-0.058	-0.320	.712*	1.000	-0.262
		Sig. (2-tailed)	0.891	0.439	0.048		0.531
		N	8	8	8	8	8
	SYP_Tumor_Cytoplasmic	Correlation Coefficient	0.317	.735*	-0.466	-0.262	1.000
		Sig. (2-tailed)	0.444	0.038	0.244	0.531	
		N	8	8	8	8	8

*. Correlation is significant at the 0.05 level (2-tailed).

A.

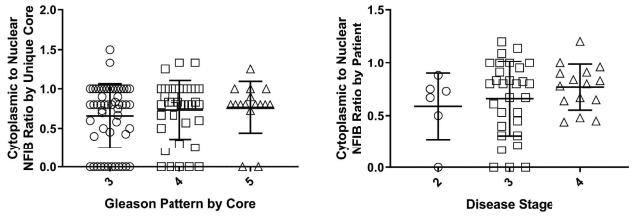
Cytoplasmic to Nuclear NFIB Ratio by Unique Core
Gleason Pattern by Core
Cytoplasmic to Nuclear NFIB Ratio by Patient
Disease Stage

B.

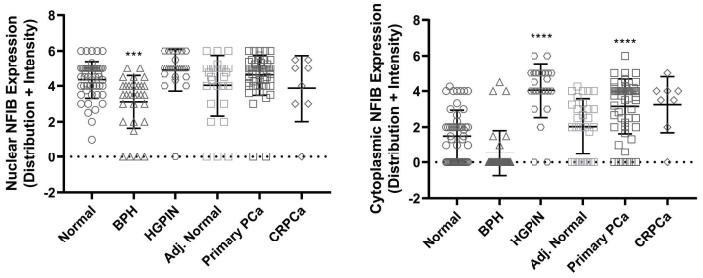
Nuclear NFIB Expression (Distribution + Intensity)
Cytoplasmic NFIB Expression (Distribution + Intensity)
Normal
BPH
HGPIN
Adj. Normal
Primary PCa
CRPCa

C.

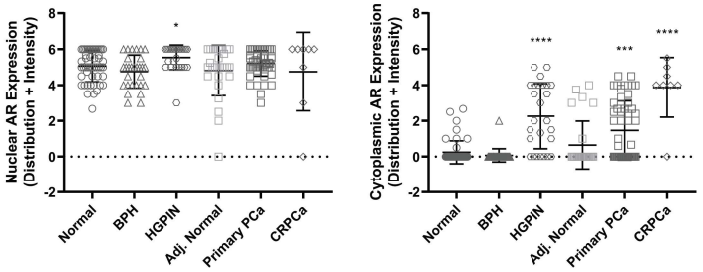
Nuclear AR Expression (Distribution + Intensity)
Cytoplasmic AR Expression (Distribution + Intensity)
Normal
BPH
HGPIN
Adj. Normal
Primary PCa
CRPCa

D.

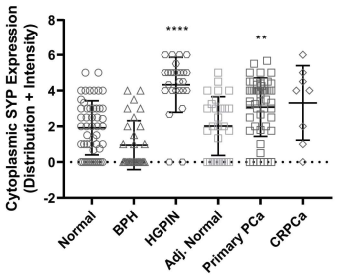
Cytoplasmic SYP Expression (Distribution + Intensity)
Normal
BPH
HGPIN
Adj. Normal
Primary PCa
CRPCa

A.

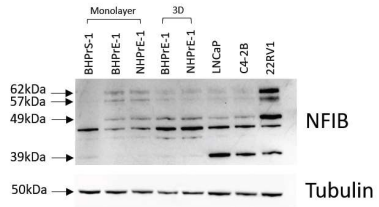

B.

NFIB bands on gels	Observed molecular weight range	Mean molecular weight
Band 1	60.5 kDa to 65 kDa	62kDa
Band 2	54.7 kDa to 60 kDa	56.98 kDa
Band 3	47.5 kDa to 50.2 kDa	48.78 kDa
Band 4	37 kDa to 40 kDa	39.2 kDa

C.

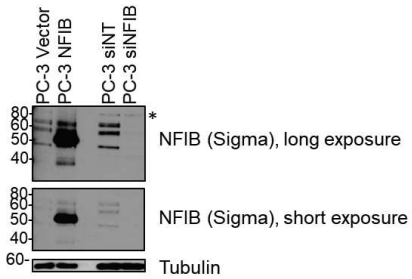
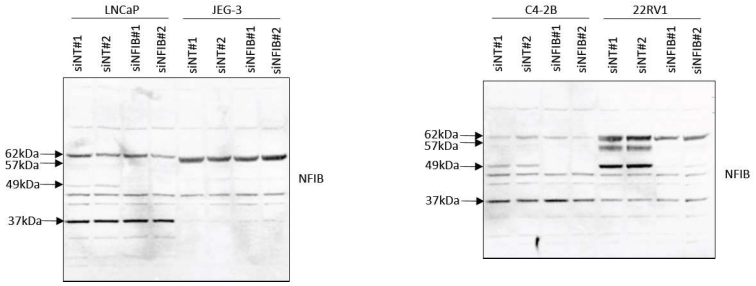
D.